

Effect of one-, two-, and three-body atom loss processes on superpositions of phase states in Bose-Josephson junctions

D. Spehner,^{1,2,*} K. Pawłowski,^{3,4,5} G. Ferrini,⁶ and A. Minguzzi²

¹*Université Grenoble 1 and CNRS, Institut Fourier UMR5582, B.P. 74, 38402 Saint Martin d'Hères, France*

²*Université Grenoble 1 and CNRS, Laboratoire de Physique et Modélisation des Milieux Condensés UMR5493, B.P. 166, 38042 Grenoble, France*

³*Center for Theoretical Physics PAN, Al. Lotników 32/46, 02-668 Warsaw, Poland*

⁴*Physikalisches Institut, Universität Stuttgart, Pfaffenwaldring 57, D-70569 Stuttgart, Germany*

⁵*Laboratoire Kastler Brossel, Ecole Normale Supérieure, 45, rue d'Ulm, 75231 Paris, France*

⁶*Laboratoire Kastler Brossel, Université Pierre et Marie Curie, 4 place de Jussieu, 75000 Paris, France*

(Dated: May 20, 2019)

In a two-mode Bose-Josephson junction formed by a binary mixture of ultracold atoms, macroscopic superpositions of phase states are produced during the time evolution after a sudden quench to zero of the coupling amplitude. Using quantum trajectories and an exact diagonalization of the master equation, we study the effect of one-, two-, and three-body atom losses on the superpositions by analyzing separately the amount of quantum correlations in each subspace with fixed atom number. The quantum correlations useful for atom interferometry are estimated using the quantum Fisher information. We identify the choice of parameters leading to the largest Fisher information, thereby showing that, for all kinds of loss processes, quantum correlations can be partially protected from decoherence when the losses are strongly asymmetric in the two modes.

PACS numbers: 03.75Gg, 42.50.Lc, 03.75.Mn, 67.85.Hj

I. INTRODUCTION

Non-classical states such as squeezed states and macroscopic superpositions of coherent states are particularly interesting for high-precision interferometry since they allow for phase resolution beyond the standard quantum limit. One of the systems where such states may be engineered is a Bose-Einstein condensate (BEC) made of metastable vapors of ultracold atoms. This system displays a wide tunability of parameters: the interaction between atoms can be controlled by Feshbach resonances [1, 2], and, by using optical lattices, the BEC can be coherently split into up to few thousands sub-systems with controlled tunneling between them [3–5]. When the atoms of the BEC are trapped in a double-well potential, they realize an external Bose-Josephson junction (BJJ). The two spatial wave functions localized inside one of the wells constitute the two modes of the BJJ and the tunneling between the wells leads to an inter-mode coupling. A BEC in a single harmonic trap of atoms in two hyperfine states resonantly coupled by a microwave radio-frequency field forms an internal BJJ. In both cases, when inter-mode coupling dominates interactions, the ground state of the BJJ is a spin coherent state (CS), that is, a product state in which all atoms are in the same superposition of the two modes. After a sudden quench to zero of the coupling, the dynamical evolution builds up entangled states because of the interactions between atoms. In the absence of decoherence mechanisms, the system evolves first into squeezed states [6–8], then to multi-component

superpositions of CSs [9, 10], and then has a revival in the initial CS.

To date, only squeezed states, which appear at times much shorter than the revival time, have been realized experimentally [11–13]. At longer times, recombination and collision processes leading to particle losses produce heating and the disappearance of the BEC. Particle losses also destroy partially the coherence of the squeezed states. This has been analyzed quantitatively in [14–17], as well as the impact of the phase noise produced by magnetic fluctuations in internal BJJs [12, 18]. The superpositions of CSs appear later in the unitary evolution and are expected to be more fragile than squeezed states. The main theoretical focus on decoherence effects on these superpositions concerns the influence of the coupling of the atoms with the electromagnetic vacuum [19] and of phase noise [20]. In particular, it has been shown in [18, 20] that the coherences of the superpositions are not strongly degraded by phase noise, and this degradation does not increase with the number of atoms in the BJJ. Under current experimental conditions photon scattering is typically negligible and phase noise can be decreased by using a spin-echo technique [13]. In such conditions, the most important sources of decoherence are particle losses. Three kinds of loss processes may play a role: one-body losses, due to inelastic collisions between trapped atoms and the background gas; two-body losses, resulting from scattering of two atoms in the magnetic trap, which changes their spin and gives them enough kinetic energy to be ejected from the trap; and three-body losses, where a three-body collision event produces a molecule and ejects a third atom out of the trap.

In a previous work [21] we have analyzed the impact of two-body losses on macroscopic superpositions produced

* Dominique.Spehner@ujf-grenoble.fr

in internal BJJs. In this paper, we extend this analysis and study the combined effect of one-body, two-body, and three-body losses on the formation of mesoscopic and macroscopic superpositions. In agreement with previous results in Ref. [22], we find by using a quantum trajectory approach that for all loss processes, the fluctuations in the total atomic interaction energy produced by the random loss events lead to an effective phase noise. We show that for weak loss rates this noise is responsible for the strongest decoherence effect. The tunability of the interaction energies makes it possible to switch this effective phase noise off in the mode losing more atoms, without changing the interaction strength in the unitary dynamics, i.e. keeping the formation times of the superpositions fixed. This possibility to protect the coherence of the superposition for strongly asymmetric losses in the two modes has been already pointed out in [21] in the case of two-body losses. We show in this work that it is true for all loss processes and that for moderate loss rates it allows to obtain states which are more useful for high-precision atom interferometry than the squeezed states. This usefulness for interferometry is quantified by the quantum Fisher information F , which is related to the best phase precision achievable in one measurement according to $(\Delta\varphi)_{\text{best}} = 1/\sqrt{F}$ [23]. We calculate the Fisher information as a function of time in the lossy BJJ by using an exact diagonalization of the master equation.

The paper is organized as follows. In Sec. II and III we introduce the master equation describing the dynamics of BJJs in the presence of particle losses and recall the definition of the quantum Fisher information. The quantum trajectory approach is described in Sec. IV. We present our main results on the time evolution of the Fisher information in a lossy BJJ in Sec. V. In order to understand these results, we analyze separately the contributions to the total atomic density matrix of quantum trajectories which do not experience any loss in Sec. VI and of trajectories having a single or several loss events in Secs. VII and VIII. The last section IX contains a summary and conclusive remarks. Four appendices offer some additional technical details.

II. QUENCHED DYNAMICS OF A BOSE-JOSEPHSON JUNCTION

In this section we first recall the main features of the dynamics of a two-mode Bose-Josephson junction (BJJ) in the quantum regime after a sudden quench of the inter-mode coupling to zero. We then introduce the Markovian master equation describing atom losses in the BJJ.

A. Initial coherent state and Husimi distribution

We denote by \hat{a}_i , \hat{a}_i^\dagger , and $\hat{n}_i = \hat{a}_i^\dagger \hat{a}_i$ the bosonic annihilation, creation, and number operators in mode $i = 1, 2$. The total number of atoms in the BJJ is given by the

operator $\hat{N} = \hat{n}_1 + \hat{n}_2$. The Fock states $|n_1, n_2\rangle$ are the joint eigenstates of \hat{n}_1 and \hat{n}_2 with eigenvalues n_1 and n_2 , respectively. Initially, the BJJ is in its ground state in the regime where inter-mode coupling dominates interactions. This initial state is well approximated by

$$|\psi(0)\rangle = |N_0; \phi = 0\rangle \equiv |N_0; \theta = \frac{\pi}{2}, \phi = 0\rangle, \quad (1)$$

where N_0 is the initial number of atoms and

$$|N; \theta, \phi\rangle = \sum_{n_1=0}^N \binom{N}{n_1}^{1/2} \frac{(\tan(\theta/2))^{n_1}}{[1 + \tan^2(\theta/2)]^{N/2}} e^{-in_1\phi} |n_1, n_2 = N - n_1\rangle \quad (2)$$

are the SU(2)-coherent states (CSs) for N atoms [24].

An arbitrary (pure or mixed) state $\hat{\rho}$ with N atoms can be represented by its Husimi distribution on the Bloch sphere of radius $N/2$,

$$Q_N(\theta, \phi) = \frac{1}{\pi} \langle N; \theta, \phi | \hat{\rho} | N; \theta, \phi \rangle.$$

This distribution provides a useful information on the phase content of $\hat{\rho}$. The initial CS (1) has a Husimi distribution with a single peak at $(\theta, \phi) = (\frac{\pi}{2}, 0)$ of width $\approx 1/\sqrt{N_0}$, as shown in the panel (a) of Fig. 1.

B. Dynamics in the absence of atom losses

After a sudden quench to zero of the inter-mode coupling at time $t = 0$, the two-mode Bose-Hubbard Hamiltonian of the atoms reads [25]

$$\hat{H}_0 = \sum_{i=1,2} \left(E_i \hat{n}_i + \frac{U_i}{2} \hat{n}_i (\hat{n}_i - 1) \right) + U_{12} \hat{n}_1 \hat{n}_2, \quad (3)$$

where E_i is the energy of the mode i , U_i the interaction energy between atoms in the same mode i , and U_{12} the interaction energy between atoms in different modes ($U_{12} = 0$ for external BJJs). For a fixed total number of atoms $N_0 = \hat{n}_1 + \hat{n}_2$, the Hamiltonian (3) has a quadratic term in the relative number operator $\hat{n}_1 - \hat{n}_2$ of the form $\chi(\hat{n}_1 - \hat{n}_2)^2/4$, with the effective interaction energy

$$\chi = \frac{U_1 + U_2 - 2U_{12}}{2}. \quad (4)$$

The atomic state $|\psi^{(0)}(t)\rangle = e^{-it\hat{H}_0} |\psi(0)\rangle$ displays a periodic evolution with period $T = 2\pi/\chi$ if N_0 is even and $T/2$ if N_0 is odd. Before the revival, the dynamics drives the system first into squeezed states at times $t \approx TN_0^{-\frac{2}{3}}$ [6] (see panel (b) in Fig. 1). At the later times

$$t_q = \frac{\pi}{\chi q} = \frac{T}{2q}, \quad q = 2, 3, \dots, \quad (5)$$

the atoms are in macroscopic superpositions of CSs

$$|\psi^{(0)}(t_q)\rangle = \sum_{k=0}^{q-1} c_{k,q} |N_0; \phi_{k,q}\rangle, \quad (6)$$

with coefficients $c_{k,q}$ of equal moduli $q^{-1/2}$ and phases $\theta = \pi/2$ and $\phi_{k,q} = \phi_{0,q} + 2\pi k/q$, where $\phi_{0,q}$ depends on q , N_0 , and the energies E_i and U_i [9, 10]. In particular, at time $t = t_2$ the BJJ is in the superposition $(|N_0; \phi_{0,2}\rangle - |N_0; \phi_{1,2}\rangle)/\sqrt{2}$ of two CSs located on the equator of the Bloch sphere at diametrically opposite points. Panels (c) and (d) of Fig. 1 show the Husimi distribution of the states (6) for $q = 2$ and $q = 3$.

It is easy to determine the matrix elements of the density matrix $\hat{\rho}^{(0)}(t) = |\psi^{(0)}(t)\rangle\langle\psi^{(0)}(t)|$ in the Fock basis. They have time-independent moduli

$$|\langle n_1, n_2 | \hat{\rho}^{(0)}(t) | n'_1, n'_2 \rangle| = \frac{1}{2^{N_0}} \binom{N_0}{n_1}^{1/2} \binom{N_0}{n'_1}^{1/2} \quad (7)$$

behaving in the limit $N_0 \gg 1$ like

$$\sqrt{\frac{2}{\pi N_0}} \exp\left\{-\frac{1}{N_0} \left((n_1 - \frac{N_0}{2})^2 + (n'_1 - \frac{N_0}{2})^2 \right)\right\}, \quad (8)$$

where we have set $n_2 = N_0 - n_1$ and $n'_2 = N_0 - n'_1$.

At the time t_q of formation of a macroscopic superposition (6), it is convenient to decompose $\hat{\rho}^{(0)}(t_q)$ as a sum of a ‘‘diagonal part’’ $[\hat{\rho}^{(0)}(t_q)]_d$, corresponding to the statistical mixture of the CSs in the superposition, and an ‘‘off-diagonal part’’ $[\hat{\rho}^{(0)}(t_q)]_{od}$ describing the coherences between these CSs. Defining $[\hat{\rho}^{(0)}(t_q)]_{kk'} = c_{k,q} c_{k',q}^* |N_0; \phi_{k,q}\rangle\langle N_0; \phi_{k',q}|$, one has [18]

$$\begin{aligned} [\hat{\rho}^{(0)}(t_q)]_d &= \sum_{k=0}^{q-1} [\hat{\rho}^{(0)}(t_q)]_{kk} \\ [\hat{\rho}^{(0)}(t_q)]_{od} &= \sum_{k \neq k'=0}^{q-1} [\hat{\rho}^{(0)}(t_q)]_{kk'}. \end{aligned} \quad (9)$$

These diagonal and off-diagonal parts exhibit remarkable structures in the Fock basis, which allow to read them easily from the total density matrix [18]:

$$\begin{aligned} \langle n_1, n_2 | [\hat{\rho}^{(0)}(t_q)]_d | n'_1, n'_2 \rangle &= 0 \text{ if } n'_1 \neq n_1 \text{ modulo } q \\ \langle n_1, n_2 | [\hat{\rho}^{(0)}(t_q)]_{od} | n'_1, n'_2 \rangle &= 0 \text{ if } n'_1 = n_1 \text{ modulo } q. \end{aligned} \quad (10)$$

The off-diagonal part does almost not contribute to the Husimi distribution. The Husimi plots in Fig. 1 (c,d) thus essentially show the diagonal parts only. On the other hand, the QCs useful for interferometry (i.e. giving rise to high value of the Fisher information, see below) are contained in the off-diagonal part $[\hat{\rho}^{(0)}(t_q)]_{od}$ [18], .

C. Master equation in the presence of atom losses

We account for loss processes in the BJJ by considering the Markovian master equation [26–28]

$$\frac{d\hat{\rho}}{dt} = -i[\hat{H}_0, \hat{\rho}(t)] + (\mathcal{L}_{1\text{-body}} + \mathcal{L}_{2\text{-body}} + \mathcal{L}_{3\text{-body}})(\hat{\rho}(t)) \quad (11)$$

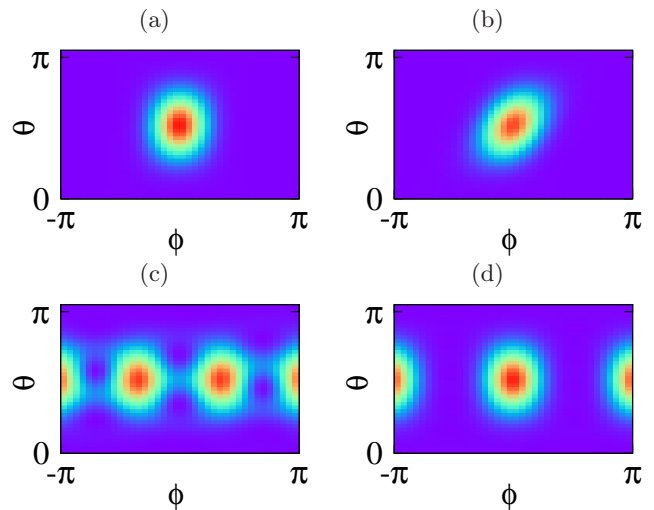


FIG. 1. (Color online) Husimi functions in the absence of losses in the BJJ at some specific times: (a) $t = 0$ (coherent state); (b) $t = T/40$ (spin squeezed state), (c) $t = T/6$ (3-component superposition of phase states), (d) $t = T/4$ (2-component superposition). Other parameters: $U_1 = U_2 = \frac{2\pi}{T}$, $U_{12} = 0$, $E_1 = E_2 = 0$, and $N_0 = 10$.

where we have set $\hbar = 1$, $\hat{\rho}(t)$ is the atomic density matrix, and the superoperators $\mathcal{L}_{1\text{-body}}$, $\mathcal{L}_{2\text{-body}}$, and $\mathcal{L}_{3\text{-body}}$ describe one-body, two-body, and three-body losses, respectively. They are given by

$$\begin{aligned} \mathcal{L}_{1\text{-body}}(\hat{\rho}) &= \sum_{i=1,2} \alpha_i \left(\hat{a}_i \hat{\rho} \hat{a}_i^\dagger - \frac{1}{2} \{ \hat{n}_i, \hat{\rho} \} \right) \\ \mathcal{L}_{2\text{-body}}(\hat{\rho}) &= \sum_{1 \leq i < j \leq 2} \gamma_{ij} \left(\hat{a}_i \hat{a}_j \hat{\rho} \hat{a}_i^\dagger \hat{a}_j^\dagger - \frac{1}{2} \{ \hat{a}_i^\dagger \hat{a}_j^\dagger \hat{a}_i \hat{a}_j, \hat{\rho} \} \right) \\ \mathcal{L}_{3\text{-body}}(\hat{\rho}) &= \sum_{1 \leq i < j < k \leq 2} \kappa_{ijk} \left(\hat{a}_i \hat{a}_j \hat{a}_k \hat{\rho} \hat{a}_i^\dagger \hat{a}_j^\dagger \hat{a}_k^\dagger \right. \\ &\quad \left. - \frac{1}{2} \{ \hat{a}_i^\dagger \hat{a}_j^\dagger \hat{a}_k^\dagger \hat{a}_i \hat{a}_j \hat{a}_k, \hat{\rho} \} \right) \end{aligned} \quad (12)$$

where the rates α_i , γ_{ij} , and κ_{ijk} correspond to the loss of one atom in the mode i , of two atoms in the modes i and j , and of three atoms in the modes i , j , and k (with $i, j, k = 1, 2$), respectively, and $\{ \cdot, \cdot \}$ denotes the anti-commutator. To shorten notation we write the loss rate of two (three) atoms in the same mode i as $\gamma_i = \gamma_{ii}$ ($\kappa_i = \kappa_{iii}$) and set $\kappa_{12} = \kappa_{112}$ and $\kappa_{21} = \kappa_{122}$. Note that the inter-mode rates γ_{12} , κ_{12} , and κ_{21} vanish for external BJJs. The loss rates depend on the macroscopic wave function of the condensate and thus on the number of atoms and interactions energies U_i . As far as the number of lost atoms at the revival time T remains small with respect to the initial number of atoms N_0 , one may assume that these rates are time-independent in the time interval $[0, T]$.

D. Conditional states

The master equation (11) does not couple sectors with different numbers of atoms. As a result, if the density matrix $\hat{\rho}(t)$ has initially no coherences between states with different atom numbers then such coherences are absent at all times $t \geq 0$. Hence

$$\hat{\rho}(t) = \sum_{N=0}^{N_0} \tilde{\rho}_N(t) \quad , \quad \tilde{\rho}_N(t) = w_N(t) \hat{\rho}_N(t) \quad , \quad (13)$$

where $\tilde{\rho}_N(t)$ ($\hat{\rho}_N(t)$) is the unnormalized (normalized) density matrix with a well-defined number of atoms N (that is, $\langle n_1, n_2 | \tilde{\rho}_N(t) | n'_1, n'_2 \rangle = 0$ for $n_1 + n_2 \neq N$ or $n'_1 + n'_2 \neq N$) and $w_N(t) \geq 0$ is probability of finding N atoms in the BJJ (thus $\sum_N w_N(t) = 1$). The matrix $\hat{\rho}_N(t)$ is the conditional state following a measurement of \hat{N} . More precisely, it describes the state of the BJJ when one selects among many single-run experiments those for which the measured atom number at time t is equal to N and one averages all experimental results over these “post-selected” single-run experiments, disregarding all the others. In this sense, $\hat{\rho}_N(t)$ contains a more precise physical information than the total density matrix $\hat{\rho}(t)$. To have access to this information, one must be able to extract samples with a well-defined number of atoms initially (since we assumed an initial state with N_0 atoms) and after the evolution time t . Even though the precise measurement of \hat{N} is still an experimental challenge, the precision has increased by orders of magnitude during the last years [29–31].

III. QUANTUM CORRELATIONS USEFUL FOR INTERFEROMETRY

A useful quantity characterizing quantum correlations (QCs) between atoms in systems involving many atoms is the quantum Fisher information. Let us recall briefly its definition and its link with phase estimation in atom interferometry (see [18, 32, 33] for more details). In a Mach-Zehnder atom interferometer, an input state $\hat{\rho}_{\text{in}}$ is first transformed into a superposition of two modes, analogous to the two arms of an optical interferometer. These modes acquire distinct phases φ_1 and φ_2 during the subsequent quantum evolution and are finally recombined to read out interference fringes, from which the phase shift $\varphi = \varphi_1 - \varphi_2$ is inferred. The output state of the interferometer is $\hat{\rho}_{\text{out}}(\varphi) = e^{-i\varphi \hat{J}_{\vec{n}}} \hat{\rho}_{\text{in}} e^{i\varphi \hat{J}_{\vec{n}}}$, where $\hat{J}_{\vec{n}} = n_x \hat{J}_x + n_y \hat{J}_y + n_z \hat{J}_z$ is the angular momentum generating a rotation on the Bloch sphere in the direction \vec{n} , with $\hat{J}_x = (\hat{a}_1^\dagger \hat{a}_2 + \hat{a}_2^\dagger \hat{a}_1)/2$, $\hat{J}_y = -i(\hat{a}_1^\dagger \hat{a}_2 - \hat{a}_2^\dagger \hat{a}_1)/2$, and $\hat{J}_z = (\hat{a}_1^\dagger \hat{a}_1 - \hat{a}_2^\dagger \hat{a}_2)/2$. The phase shift φ is determined by means of a statistical estimator depending on the results of measurements on the output state $\hat{\rho}_{\text{out}}(\varphi)$. The best precision on φ that can be achieved (that is, optimizing over all possible estimators and measurements) is given

when $|\varphi| \ll 1$ by [23]

$$(\Delta\varphi)_{\text{best}} = \frac{1}{\sqrt{\mathcal{M} F(\hat{\rho}_{\text{in}}, \hat{J}_{\vec{n}})}} \quad , \quad (14)$$

where \mathcal{M} is the number of measurements and

$$F(\hat{\rho}, \hat{J}_{\vec{n}}) = 2 \sum_{k,l,p_k+p_l>0} \frac{(p_k - p_l)^2}{p_k + p_l} |\langle k | \hat{J}_{\vec{n}} | l \rangle|^2 \quad (15)$$

is the quantum Fisher information. Here, $\{|l\rangle\}$ is an orthonormal basis diagonalizing $\hat{\rho}$, $\hat{\rho}|l\rangle = p_l|l\rangle$. The quantum Fisher information thus measures the amount of QCs in the input state that can be used to enhance phase sensitivity with respect to the shot noise limit $(\Delta\varphi)_{\text{SN}} = 1/\sqrt{\mathcal{M} \langle \hat{N} \rangle}$, that is, to the sensitivity obtained by using $\langle \hat{N} \rangle$ independent atoms. Since $\hat{J}_{\vec{n}}$ does not couple subspaces with different N 's, it follows from Eq.(15) and from the block structure (13) of $\hat{\rho}$ that

$$F(\hat{\rho}, \hat{J}_{\vec{n}}) = \sum_{N=0}^{N_0} w_N F(\hat{\rho}_N, \hat{J}_{\vec{n}}) \quad , \quad (16)$$

where $F_N(\hat{\rho}_N, \hat{J}_{\vec{n}})$ is the Fisher information associated to the conditional state $\hat{\rho}_N$ with N atoms and w_N is the corresponding probability.

It is shown in [34] that if $F(\hat{\rho}, \hat{J}_{\vec{n}})$ is larger than the average number of atoms $\langle \hat{N} \rangle$ then the atoms are entangled. According to Eq.(14), the condition $F(\hat{\rho}, \hat{J}_{\vec{n}}) > \langle \hat{N} \rangle$ is a necessary and sufficient condition for sub-shot noise sensitivity $(\Delta\varphi)_{\text{best}} < (\Delta\varphi)_{\text{SN}}$.

In order to obtain a measure of QCs independent of the direction \vec{n} of the interferometer, we optimize the Fisher information over all unit vectors \vec{n} and define [35],

$$F(\hat{\rho}(t)) = \max_{\|\vec{n}\|=1} F(\hat{\rho}(t), \hat{J}_{\vec{n}}) = 4C_{\text{max}} \quad . \quad (17)$$

Here, C_{max} is the largest eigenvalue of the 3×3 real symmetric covariance matrix

$$C_{ab} = \frac{1}{2} \sum_{k,l,p_k+p_l>0} \frac{(p_k - p_l)^2}{p_k + p_l} \text{Re} \{ \langle k | \hat{J}_a | l \rangle \langle l | \hat{J}_b | k \rangle \} \quad , \quad (18)$$

$a, b = 1, 2, 3$. For simplicity we write $F_{\text{tot}}(t) \equiv F(\hat{\rho}(t))$ for the optimized total Fisher information (17). When studying the QCs in the conditional states $\hat{\rho}_N(t)$, we optimize over \vec{n} independently in each subspace and define $F_N(t) = \max_{\|\vec{n}\|=1} F(\hat{\rho}_N(t), \hat{J}_{\vec{n}})$. Note that $F_{\text{tot}}(t)$ is not equal to $\sum_N w_N(t) F_N(t)$, because the optimal directions may be different in each subspace.

In the absence of losses, the two-component superposition of CSs has the highest possible Fisher information $F[\hat{\rho}^{(0)}(t_2)] = N_0^2$, which is for $N_0 \gg 1$ approximately twice larger than that of the superpositions with q components, $3 \leq q \lesssim N_0^{1/2}$ [18, 33]. The upper solid curve in Fig. 2 shows $F_{\text{tot}}(t)$ in the absence of losses as a function of time for $N_0 = 10$ atoms in the BJJ.

IV. QUANTUM TRAJECTORIES

We solve the master equation (11) using two methods: the quantum jump approach and an exact diagonalization. We outline in this section the quantum jump approach. It yields a tractable analytical solution in the case of few loss events and allows to gain physical intuition on the various mechanisms leading to decoherence. It will be used to explain the results provided by the exact diagonalization method. The latter offers the exact but complex solution for the whole density matrix when the inter-mode losses are absent, i.e. $\gamma_{12} = \kappa_{21} = \kappa_{12} = 0$. We use it mostly to compute numerically the Fisher information. The details of the exact diagonalization are given in Appendix A.

In the quantum jump description, the state of the atoms is a pure state $|\psi(t)\rangle$ which evolves randomly in time as follows [36–41]. At random times s quantum jumps occur and the atomic state is transformed as

$$|\psi(s-)\rangle \longrightarrow |\psi(s+)\rangle = \frac{\hat{M}_m |\psi(s-)\rangle}{\|\hat{M}_m |\psi(s-)\rangle\|}, \quad (19)$$

where the index m labels the type of jump and \hat{M}_m is the corresponding jump operator. In our case, restricting for the moment our attention to two-body losses, one has three types of jumps: the loss of two atoms in the first mode, with $\hat{M}_{2,0} = \hat{a}_1^2$, the loss of two atoms in the second mode, with $\hat{M}_{0,2} = \hat{a}_2^2$, and the loss of one atom in each mode, with $\hat{M}_{1,1} = \hat{a}_1 \hat{a}_2$. The probability that a jump m occurs in the infinitesimal time interval $[s, s + ds]$ is $dp_m(s) = \Gamma_m \|\hat{M}_m |\psi(s)\rangle\|^2 ds$, where Γ_m is the jump rate in the loss channel m . Using the notation of Sec. II C, one has $\Gamma_{2,0} = \gamma_1$, $\Gamma_{0,2} = \gamma_2$, and $\Gamma_{1,1} = \gamma_{12}$. Between jumps, the wave function $|\psi(t)\rangle$ evolves according to the effective non self-adjoint Hamiltonian $\hat{H}_{\text{eff}} = \hat{H}_0 - i\hat{D}_{2\text{-body}}$ with

$$\begin{aligned} \hat{D}_{2\text{-body}} &= \frac{1}{2} \sum_m \Gamma_m \hat{M}_m^\dagger \hat{M}_m \\ &= \frac{1}{2} \sum_{i=1,2} \gamma_i \hat{n}_i (\hat{n}_i - 1) + \frac{\gamma_{12}}{2} \hat{n}_1 \hat{n}_2. \end{aligned} \quad (20)$$

The physical origin of the damping term relies on the gain of information acquired on the atomic state from conditioning the system to have no loss in a given time interval [37, 41]: the longer the time interval, the smaller must be the number of atoms left in the BJJ in the mode losing atoms.

The random wave function at time t reads

$$\begin{aligned} |\psi_J(t)\rangle &= \frac{|\tilde{\psi}_J(t)\rangle}{\|\tilde{\psi}_J(t)\rangle} \\ |\tilde{\psi}_J(t)\rangle &= e^{-i(t-s_J)\hat{H}_{\text{eff}}} \hat{M}_{m_J} e^{-i(s_J-s_{J-1})\hat{H}_{\text{eff}}} \hat{M}_{m_{J-1}} \cdots \\ &\quad \cdots e^{-i\hat{H}_{\text{eff}}(s_2-s_1)} \hat{M}_{m_1} e^{-is_1\hat{H}_{\text{eff}}} |\psi(0)\rangle \end{aligned} \quad (21)$$

where J is the number of loss events in the time interval $[0, t]$, $0 \leq s_1 \leq \cdots \leq s_J \leq t$ are the random loss

times, and m_1, \dots, m_J the random loss types. The time evolution of the wave function $t \mapsto |\psi_J(t)\rangle$ for a fixed realization of the jump process is called a quantum trajectory.

The probability to have no atom loss between times 0 and t is given by $\|e^{-it\hat{H}_{\text{eff}}} |\psi(0)\rangle\|^2$. The probability to have J loss events in $[0, t]$, with the ν th event occurring in the time interval $[s_\nu, s_\nu + ds_\nu]$, $\nu = 1, \dots, J$, is

$$\begin{aligned} dp_{m_1, \dots, m_J}^{(t)}(s_1, \dots, s_J; J) \\ = \Gamma_{m_1} \cdots \Gamma_{m_J} \|\tilde{\psi}_J(t)\|^2 ds_1 \cdots ds_J. \end{aligned} \quad (22)$$

The link of this approach with the master equation description is that the average over all quantum trajectories (that is, over the number of jumps J , the jump times s_ν , and the jump types m_ν) of the rank-one projector $|\psi_J(t)\rangle\langle\psi_J(t)|$ yields the density matrix $\hat{\rho}(t)$ solution of the master equation (11) [37]. We thus recover the block structure (13) of the atom density matrix, with

$$\begin{aligned} \tilde{\rho}_{N_J}(t) &= \sum_{m_1, \dots, m_J} \Gamma_{m_1} \cdots \Gamma_{m_J} \int_{0 \leq s_1 \leq \cdots \leq s_J \leq t} ds_1 \cdots ds_J \\ &\quad |\tilde{\psi}_J(t)\rangle\langle\tilde{\psi}_J(t)| \end{aligned} \quad (23)$$

and $N_J = N_0 - 2J$. Therefore, quantum trajectories provide a natural and efficient tool to study the conditional states $\tilde{\rho}_{N_J}(t)$ with N_J atoms, which only depend on quantum trajectories having J two-body loss events.

It is straightforward to extend the above description to include also one-body and three-body losses. This is achieved by adding new types of jumps with jump operators $\hat{M}_{1,0} = \hat{a}_1$, $\hat{M}_{0,1} = \hat{a}_2$ (for one-body losses) and $\hat{M}_{3,0} = \hat{a}_1^3$, $\hat{M}_{0,3} = \hat{a}_2^3$, $\hat{M}_{2,1} = \hat{a}_1^2 \hat{a}_2$, and $\hat{M}_{1,2} = \hat{a}_1 \hat{a}_2^2$ (for three-body losses). The corresponding jump rates are $\Gamma_{1,0} = \alpha_1$, $\Gamma_{0,1} = \alpha_2$, $\Gamma_{3,0} = \kappa_1$, $\Gamma_{0,3} = \kappa_2$, $\Gamma_{2,1} = \kappa_{12}$, and $\Gamma_{1,2} = \kappa_{21}$. The conditional state $\hat{\rho}_N(t)$ is obtained by summing the right-hand side of Eq.(23) over all J and all $r_1, \dots, r_J \in \{1, 2, 3\}$ such that $N_0 - \sum_{\nu=1}^J r_\nu = N$, r_ν being the number of atoms lost in the ν th loss event. The effective Hamiltonian becomes $\hat{H}_{\text{eff}} = \hat{H}_0 - i\hat{D}$ with $\hat{D} = \hat{D}_{1\text{-body}} + \hat{D}_{2\text{-body}} + \hat{D}_{3\text{-body}}$ and

$$\hat{D}_{1\text{-body}} = \frac{1}{2} \sum_{i=1,2} \alpha_i \hat{n}_i \quad (24)$$

$$\begin{aligned} \hat{D}_{3\text{-body}} &= \frac{1}{2} \sum_{i=1,2} \kappa_i \hat{n}_i (\hat{n}_i - 1) (\hat{n}_i - 2) \\ &\quad + \frac{1}{2} \sum_{i \neq j} \kappa_{ij} \hat{n}_i (\hat{n}_i - 1) \hat{n}_j. \end{aligned} \quad (25)$$

V. QUANTUM CORRELATIONS IN THE PRESENCE OF PARTICLE LOSSES

We present in this section our main results on the evolution of the QCs in the atomic state under the quenched

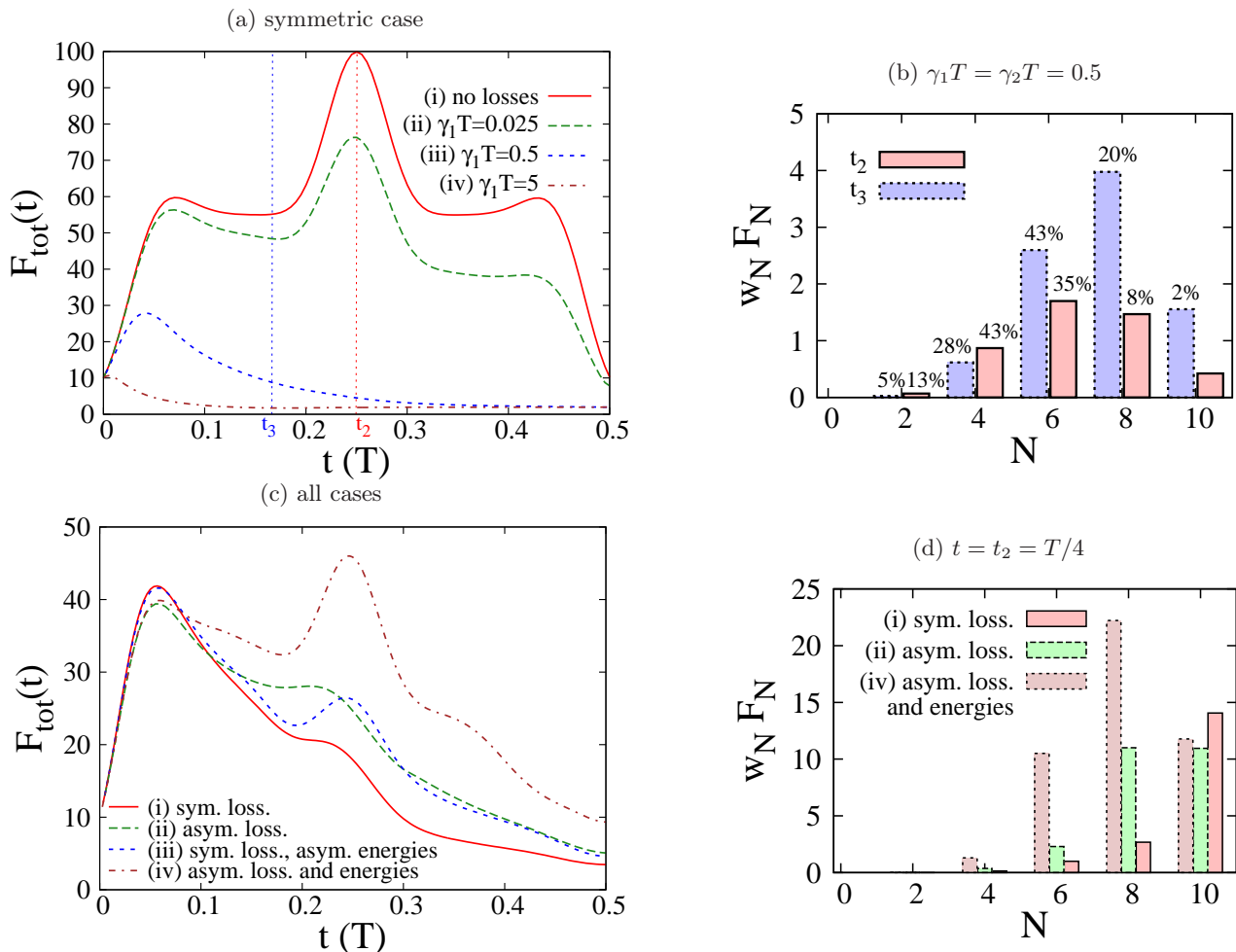


FIG. 2. (Color online) (a) Total quantum Fisher information $F_{\text{tot}}(t)$ versus time t (in units of $T = 2\pi/\chi$) for symmetric two-body loss rates $\gamma_1 = \gamma_2$ in each mode and $\gamma_{12} = \alpha_i = \kappa_i = \kappa_{ij} = 0$. The different curves correspond to (from top to bottom) $\gamma_1 T = 0, 0.025, 0.5$, and 5 . The dotted vertical lines indicate the formation times $t_2 = T/4$ and $t_3 = T/6$ of the 2-component and 3-component superpositions. The histogram (b) show the contributions $w_N F_N(\hat{\rho}_N, J_{\vec{n}_{\text{opt}}})$ to $F_{\text{tot}}(t)$ of the subspaces with different atom numbers N [see Eq.(16)] for two different times, t_2 (right pink boxes) and t_3 (left blue boxes), and for the loss rates indicated above the histogram. The percentages on top of each box are the probabilities w_N of finding N atoms at these times (weights smaller than 1% are not indicated). (c) Same as in (a) for (i) symmetric losses ($\gamma_1 = \gamma_2 = 0.177/T$) and energies ($U_1 = U_2$); (ii) asymmetric losses ($\gamma_1 = 0.6/T, \gamma_2 = 0$) and symmetric energies ($U_1 = U_2$); (iii) symmetric losses ($\gamma_1 = \gamma_2 = 0.177/T$) and asymmetric energies ($U_2 = U_{12} < U_1$); (iv) asymmetric losses ($\gamma_1 = 0, \gamma_2 = 0.6/T$) and energies ($U_2 = U_{12} < U_1$). Loss rates are chosen in such a way that the number of lost atoms at time t_2 is the same and equal to about 3 in all cases. The interaction energies U_i are such that $T = 4\pi/(U_1 + U_2 - 2U_{12})$ is the same in all cases. (d) Histogram of the contributions of the subspaces with N atoms to $F_{\text{tot}}(t)$ at the time t_2 , for the same values of γ_i and U_i as in (c) in the cases (i) (right pink boxes), (ii) (middle green boxes), and (iii) (left purple boxes). In all figures $N_0 = 10$ and $\gamma_{12} = 0$. All results are obtained from the exact diagonalization method (see Appendix A).

dynamics in the presence of atom losses. The amount of QCs is estimated by the total quantum Fisher information $F_{\text{tot}}(t)$.

Before investigating the combined effect of the various loss processes, we start by a detailed analysis of a small atomic sample with $N_0 = 10$ atoms subject to two-body losses only and without inter-mode losses (the latter losses cannot be addressed by our exact diagonalization and will be discussed in Secs. VI-VIII). In this case we can study the separate contribution of the Fisher information from all the subspaces with fixed atom number.

Figure 2 shows the effect of increasing the atom loss rates in a symmetric model $\gamma_1 = \gamma_2$ and $U_1 = U_2$ (panel (a)). The quantum Fisher information, which in the absence of losses is characterized by a large peak at the time $t = T/4$ of formation of the two-component superposition, rapidly decreases once the loss rate increases. If, however, an asymmetric model is chosen – with parameters yielding the same average number of lost atoms at time t_2 and the same revival time T as in the symmetric case – as a main result we find that the quantum Fisher information is considerably increased (panel (c) in Fig.2). The

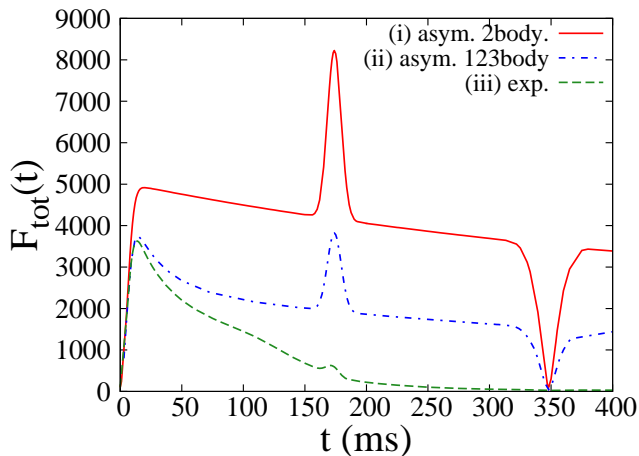


FIG. 3. (Color online) Total quantum Fisher information $F_{\text{tot}}(t)$ versus time t (in units of $T = 2\pi/\chi$) from exact diagonalization. Example for realistic experimental conditions from the papers [12, 14, 16] with $N_0 = 100$, $U_2 = U_{12}$, $U_1 - U_{12} = 18.056\text{Hz}$, and (i) symmetric two-body losses $\gamma_2 = 0.0127\text{Hz}$ and $\gamma_1 = 0$ without one- and three-body losses; (ii) one-, two-, and three-body losses in the second mode with rates $\alpha_2 = 0.4\text{Hz}$, $\gamma_2 = 0.0127\text{Hz}$, $\kappa_2 = 1.08 \times 10^{-6}\text{Hz}$ and no losses in the first mode; (iii) symmetric one- and three-body losses and asymmetric two-body losses, $\alpha_1 = \alpha_2 = 0.2\text{Hz}$, $\gamma_2 = 0.0127\text{Hz}$, $\gamma_1 = 0$, and $\kappa_1 = \kappa_2 = 0.54 \times 10^{-6}\text{Hz}$.

most favorable situation turns out to be the one with asymmetric energies $U_2 = U_{12} < U_1$ and vanishing loss rate $\gamma_1 = 0$ in the channel with largest interactions (a similar result would be obtained for $U_1 = U_{12} < U_2$ and $\gamma_2 = 0$). The histograms in panels (b) and (d) give the contributions to the total Fisher information of the various subspaces with fixed atom numbers, see (16), evaluated in the direction \vec{n}_{opt} optimizing $F(\hat{\rho}(t), \hat{J}_{\vec{n}})$. These histograms show that the aforementioned effects are non-trivial, namely, the large Fisher informations at times t_2 and t_3 for asymmetric rates and energies do not come from the contribution of the subspace with the initial atom number N_0 .

We study next an atomic sample with $N_0 = 100$ atoms initially in the case where several loss processes are combined together. Figure 3 shows the total quantum Fisher information for experimentally relevant parameters extracted from Refs. [12, 14, 16]. The precise way how these parameters are obtained can be found in Appendix B. As can be seen in Fig. 3, under two-body asymmetric losses only, the QCs of the superpositions are well preserved like in the small atomic sample discussed above. As far as two-body losses are concerned, this asymmetric situation is realized in the experiment [13], the two-body losses occurring mainly in upper internal level [42]. When one-body and three-body losses – which are also present in this experiment – are added, the coherence of the macroscopic superpositions are still preserved provided one has no loss in one mode. In this case, the QCs in the macroscopic superpositions can thus be protected

against atom losses by tuning the interaction energies U_2 such that $U_2 = U_{12}$. This shows that the results of [21] concerning two-body losses hold for one-body and three-body losses as well. However, when symmetric one-body and three-body losses are added, the QCs are destroyed on a much shorter time scale and the peak in the Fisher information at the time t_2 disappears. In the experiments [12, 13], the one-body losses are symmetric in the two modes since they are due to collisions with atoms from the background gas, which are equally likely for the two internal atomic states. This means that, if one allows for a tuning of the interaction energies, one- and three-body losses are much more detrimental to the QCs of macroscopic superpositions than two-body losses.

The purpose of the following sections is to explain the smaller effect of decoherence for strongly asymmetric loss rates and interaction energies observed in Figs. 2 and 3. To this end, we analyze separately the contribution of each subspace with a fixed atom number to the total Fisher information by using the quantum jump approach of Sec. IV, that is, we study the QCs of the conditional states $\hat{\rho}_N(t)$ with $N < N_0$ atoms. We will show that the stronger decoherence for symmetric two-body rates and energies originates from a “destructive interference” (exact cancellation) when adding the contributions of the two loss channels at time t_2 , and that a similar cancellation occurs at time t_3 for symmetric three-body losses, but is absent for one-body losses. Moreover, the weaker decoherence for asymmetric losses obtained by tuning the interaction energies as described above comes from the absence of dephasing in the mode i losing atoms. This effect is somehow trivial for external BJJs: then this absence of dephasing is obtained for a vanishing interaction energy $U_i = U_{12} = 0$; for such an energy the collision processes responsible of two-body losses in the mode i are suppressed (moreover, our assumption that the loss rates are independent of the energies is not justified anymore). In contrast, for internal BJJs decoherence is reduced when U_i is equal to the inter-mode interaction $U_{12} \neq 0$ and the effect is non-trivial. We shall explain it by invoking the effective phase noise produced by atom losses in the presence of interactions discussed in [21, 22].

VI. CONDITIONAL STATE IN THE SUBSPACE WITH THE INITIAL NUMBER OF ATOMS

In this section we determine the conditional state $\hat{\rho}_{N_0}(t)$ with N_0 atoms at time t . In the quantum jump approach this corresponds to the contribution of quantum trajectories with no jump in the time interval $[0, t]$, which are given by (see Sec. IV)

$$|\tilde{\psi}_0(t)\rangle = e^{-it(\hat{H}_0 - i\hat{D})}|N_0; \phi = 0\rangle. \quad (26)$$

The unnormalized conditional state is $\tilde{\rho}_{N_0}^{(\text{no loss})}(t) = |\tilde{\psi}_0(t)\rangle\langle\tilde{\psi}_0(t)|$. In the Fock basis diagonalizing both \hat{H}_0

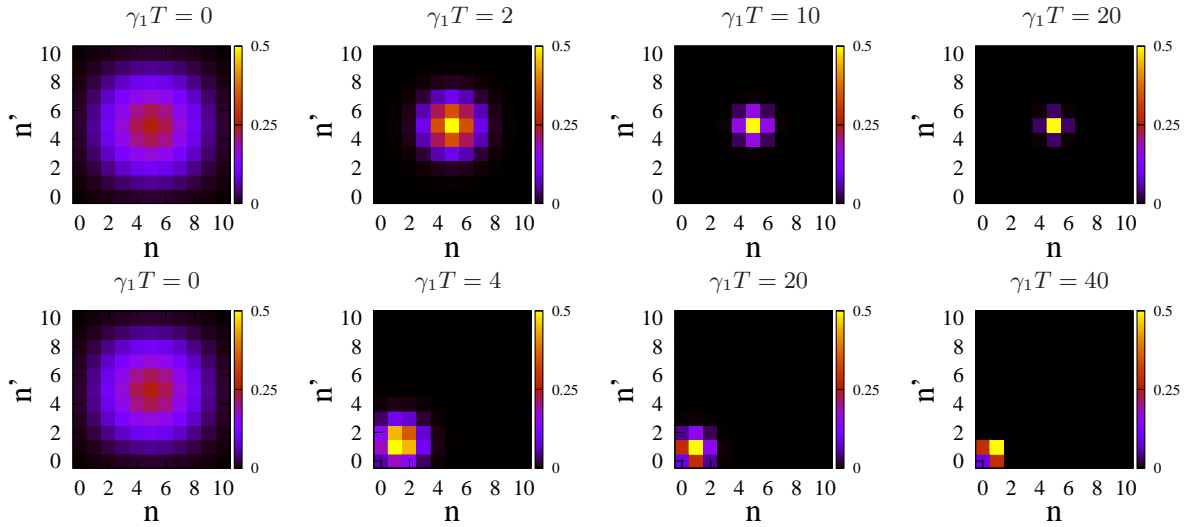


FIG. 4. (Color online) Moduli of the matrix elements in the Fock basis of the state $\hat{\rho}_{N_0}(t_3)$ in the subspace with N_0 atoms at the time of formation $t_3 = T/6$ of the 3-component superposition, from the exact diagonalization method. Upper panels: symmetric two-body loss rates ($\gamma_1 = \gamma_2$). Lower panels: completely asymmetric two-body losses ($\gamma_2 = 0$). The values of γ_1 are indicated on the top of each panel. Other parameters: $\alpha_i = \gamma_{ij} = \kappa_i = \kappa_{ij} = 0$ and $N_0 = 10$.

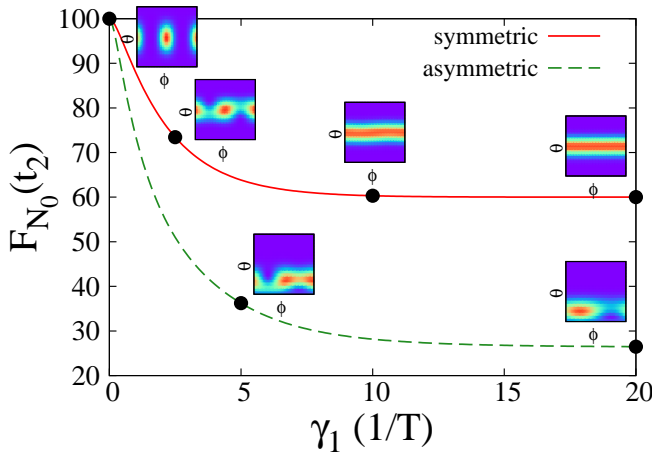


FIG. 5. (Color online) Fisher information $F_{N_0}(t_2)$ optimized in the subspace with N_0 atoms at the time t_2 of formation of the two-component superposition as a function of the loss rate γ_1 (in units of T^{-1}). Solid line: symmetric loss rates ($\gamma_1 = \gamma_2$). Dashed line: asymmetric rates ($\gamma_2 = 0$). The Husimi functions are plotted in the insets for some specific choices of loss rates indicated by circles in the two curves. Other parameters as in Fig. 4.

and \hat{D} , it takes the form

$$\langle n_1, n_2 | \hat{\rho}_{N_0}^{(\text{no loss})}(t) | n'_1, n'_2 \rangle = e^{-t[d_{N_0}(n_1) + d_{N_0}(n'_1)]} \langle n_1, n_2 | \hat{\rho}_{N_0}^{(0)}(t) | n'_1, n'_2 \rangle, \quad (27)$$

where $\hat{\rho}_{N_0}^{(0)}(t)$ is the state in the absence of losses (see Sec. II B), $n_2 = N_0 - n_1$, $n'_2 = N_0 - n'_1$, and $d_{N_0}(n_1) = \langle n_1, N_0 - n_1 | \hat{D} | n_1, N_0 - n_1 \rangle$. The probability to find N_0 atoms in the BJJ at time t is found with the help of

Eqs.(7) and (27). One finds

$$w_{N_0}(t) = \text{tr} \tilde{\rho}_{N_0}^{(\text{no loss})}(t) = \frac{1}{2^{N_0}} \sum_{n_1=0}^{N_0} \binom{N_0}{n_1} e^{-2td_{N_0}(n_1)}. \quad (28)$$

We now restrict our attention to *symmetric three-body losses* $\kappa_1 = \kappa_2$ and $\kappa_{12} = \kappa_{21}$. The asymmetric three-body loss case is treated in Appendix C. Let us set $\kappa = (3\kappa_1 - \kappa_{12})/2$ and

$$a = \frac{1}{2}(\gamma_1 + \gamma_2 - \gamma_{12}) + (N_0 - 2)\kappa. \quad (29)$$

If $a \neq 0$, the damping factor (exponential factor in the right-hand side) in Eq.(27) is Gaussian. Actually, by using Eqs.(20), (24), and (25), one obtains

$$d_{N_0}(n_1) = a(n_1 - \bar{n}_1)^2 + c, \quad (30)$$

where c is an irrelevant n_1 -independent constant (which can be absorbed in the normalization of the density matrix) and

$$\bar{n}_1 = \frac{1}{4a} (\Delta\alpha - \Delta\gamma + N_0(2\gamma_2 - \gamma_{12}) + 2N_0(N_0 - 2)\kappa) \quad (31)$$

with $\Delta\alpha = \alpha_2 - \alpha_1$ and $\Delta\gamma = \gamma_2 - \gamma_1$.

In order to estimate the QCs in $\hat{\rho}_{N_0}(t)$ and the typical loss rates at which this state is affected by the Gaussian damping, we now focus on three particular cases.

(i) *Symmetric loss rates* $\gamma_1 = \gamma_2$ and $\alpha_1 = \alpha_2$. In this case $a = \gamma/2 + (N_0 - 2)\kappa$ with $\gamma = 2\gamma_1 - \gamma_{12}$ and $\bar{n}_1 = N_0/2$. Hence the damping factor in Eq.(27) is a Gaussian centered at $(n_1, n'_1) = (N_0/2, N_0/2)$. This center coincides with the peak of the matrix elements (7) in the absence of losses, which have a width $\approx \sqrt{N_0}$, see

Eq.(8). Thus the effect of the Gaussian damping begins to set in for times t such that $at \approx 1/N_0$. In particular, the macroscopic superposition at time $t_q = \pi/(\chi q)$ is noticeably affected by damping for $a \gtrsim \chi q/N_0$. It is shown in Appendix C that $\hat{\rho}_{N_0}(t_q)$ converges at large loss rates $a \gg \chi q$ to the pure Fock state $|N_0/2, N_0/2\rangle$ with equal numbers of atoms in each mode if N_0 is even, as could be expected from the symmetry of the losses. This convergence is illustrated in the upper panels in Fig. 4, which represent the density matrix (27) at time $t = t_3$ for various symmetric two-body loss rates and vanishing one-body, three-body, and inter-mode rates. The quantum Fisher information $F_{N_0}(t_2)$ in the subspace with N_0 atoms at time t_2 is displayed in Fig. 5. For $\gamma_1 = \gamma_2 \gtrsim 5/T$, it is close to the Fisher information $F_{N_0}(\infty) = N_0(N_0/2 + 1)$ of the Fock state $|N_0/2, N_0/2\rangle$. Let us, however, stress that at such loss rates, $\hat{\rho}_{N_0}(t_2)$ has a negligible contribution to the total density matrix (13) and is very unlikely to show up in a single-run experiment, because the no-jump probability $w_{N_0}(t_2)$ is very small. The large value of $F_{N_0}(t_2)$ for strong symmetric losses does thus not mean that the total state $\hat{\rho}(t)$ has a large amount of QCs. The Husimi distributions of the conditional states $\hat{\rho}_{N_0}(t_2)$ are shown in the upper insets of Fig. 5 for various rates γ_1 . The two peaks at $(\theta, \phi) = (\pi/2, 0)$ and $(\pi/2, \pi)$ of the two-component superposition in the absence of losses are progressively washed out at increasing γ_1 , until one reaches the flat ϕ -distribution of the Fock state $|N_0/2, N_0/2\rangle$.

(ii) *Completely asymmetric two-body losses and no three-body losses*, $\gamma_2 = \gamma_{12} = \kappa = 0$. Then $a = \gamma_1/2$ and $\bar{n}_1 = \Delta\alpha/(2\gamma_1) + 1/2$. The onset of the damping on the q -component superposition is at the loss rate $\gamma_1 \approx \chi q/N_0^2$, which is smaller by a factor N_0 with respect to the symmetric case, except for strongly asymmetric one-body loss rates satisfying $\Delta\alpha \approx \gamma_1 N_0$. In the latter case, this onset occurs when $\gamma_1 \approx \chi q/N_0$ as in case (i). Therefore, if $\Delta\alpha$ is not approximately equal to $\gamma_1 N_0$, the Gaussian damping factor in Eq.(27) affects more strongly the lossless density matrix than in the symmetric case. The lower panels in Fig. 4 and dashed curve in Fig. 5 display the matrix elements of $\hat{\rho}_{N_0}(t_3)$ in the Fock basis and the Fisher information $F_{N_0}(t_2)$, respectively, for $\Delta\alpha = \kappa = 0$. Except at small values of γ_1 , $F_{N_0}(t_2)$ is much smaller than for symmetric losses. This can be explained from the results of Appendix C, showing that $\hat{\rho}_{N_0}(t_q)$ converges in the strong loss limit $\gamma_1 \gg \chi q$ to the Fock state $|0, N_0\rangle$ if $\alpha_2 < \alpha_1$ and to a superposition of Fock states with $n_1 = 0$ or 1 atoms in the first mode if $\alpha_1 = \alpha_2$. These pure states have Fisher informations $\approx N_0$ smaller by a factor N_0 than that obtained for strong symmetric losses. Because the aforementioned Fock states are localized near the south pole of the Bloch sphere ($\theta = 0$), the two peaks in the Husimi functions (lower insets in Fig. 5) move to values of θ smaller than $\pi/2$ when increasing γ_1 . Note that this picture is drastically modified when $\alpha_2 = \gamma_1 N_0 + \alpha_1$: then $\hat{\rho}_{N_0}(t_2)$ converges to a superposition of the Fock states $|N_0/2, N_0/2\rangle$

and $|N_0/2 + 1, N_0/2 + 1\rangle$ for even N_0 (see Appendix C), and thus $F_{N_0}(t_2)$ behaves like in the case (i).

(iii) *Strong inter-mode two body losses* $\gamma_{12} > \gamma_1 + \gamma_2 + 2(N_0 - 2)\kappa$, i.e. $a < 0$. Then the onset of damping at time t_q occurs for $|a| \approx \chi q/N_0^2$, excepted when $\Delta\gamma \approx -\Delta\alpha/(N_0 - 1)$, in which case it occurs for $|a| \approx \chi q/N_0$. As shown in the Appendix C, $\hat{\rho}_{N_0}(t_q)$ converges at strong losses either to the Fock state with $n_1 = 0$ or $n_1 = N_0$ atoms in the first mode, which has a Fisher information equal to N_0 , or, if $\Delta\gamma = -\Delta\alpha/(N_0 - 1)$, to the so-called NOON state, which has the highest possible Fisher information $F_{N_0}(\infty) = N_0^2$.

VII. CONDITIONAL STATES WITH $N < N_0$ ATOMS

A. Contribution of trajectories with a single loss event

We study in this subsection the contribution to the total atomic density matrix $\hat{\rho}(t)$ of quantum trajectories having exactly one jump in the time interval $[0, t]$.

Let $t \mapsto |\psi_1(t)\rangle$ be such a trajectory subject to a single loss process, occurring at time $s \in [0, t]$. We denote the type of loss process by the pair $m = (m_1, m_2) \in \{1, 2, 3\}^2$, where m_1 and m_2 are the number of atoms lost in the first and second modes, respectively. The associated jump operator is $\hat{M}_m = \hat{a}_1^{m_1} \hat{a}_2^{m_2}$ (see Sec. IV). The total number of atoms kicked out from the system at time s is denoted by $r = |m| = m_1 + m_2$. It is easy to see that the jump (19) transforms a CS $|N_0; \theta, \phi\rangle$ into a CS $|N_0 - r; \theta, \phi\rangle$. We will argue below that for three-body loss rates satisfying $N_0\kappa_{it} \ll 1$ and $N_0\kappa_{ijt} \ll 1$, this CS is rotated on the Bloch sphere by the evolution in the time intervals $[0, s]$ and $[s, t]$ driven by the nonlinear effective Hamiltonian \hat{H}_{eff} . More precisely,

$$|\psi_1(t)\rangle \propto e^{-it\hat{H}_{\text{eff}}} |N_0 - r; \theta_m(s), \phi_m(s)\rangle, \quad (32)$$

where $\theta_m(s)$ and $\phi_m(s)$ are random angles depending on the loss type m and time s . These angles are given by

$$\begin{aligned} \theta_m(s) &= 2 \arctan\left(\exp\left\{-\frac{s}{2}(\delta_1 m_1 + \delta_2 m_2)\right\}\right) \\ \phi_m(s) &= s(\chi_1 m_1 + \chi_2 m_2), \end{aligned} \quad (33)$$

where we have introduced the interaction energies

$$\chi_1 = U_1 - U_{12} \quad , \quad \chi_2 = -(U_2 - U_{12}), \quad (34)$$

and the loss rate differences

$$\begin{aligned} \delta_1 &= 2\gamma_1 - \gamma_{12} + (3\kappa_1 - \kappa_{21})N_0, \\ \delta_2 &= -(2\gamma_2 - \gamma_{12} + (3\kappa_2 - \kappa_{12})N_0). \end{aligned} \quad (35)$$

To establish this result, we first take as initial state a Fock state $|n_1, n_2\rangle$, which is an eigenstate of \hat{H}_{eff} with eigenvalue $\hat{H}_{\text{eff}}(n_1, n_2)$. According to Eq.(21), the corresponding unnormalized wave function $|\psi_1(t)\rangle$ at time t is

(up to a prefactor) a Fock state with $n'_i = n_i - m_i \geq 0$ atoms in the mode $i = 1, 2$,

$$\begin{aligned} |\tilde{\psi}_1(t)\rangle &= e^{-i(t-s)\hat{H}_{\text{eff}}}\hat{M}_m e^{-is\hat{H}_{\text{eff}}}|n_1, n_2\rangle \\ &= \sqrt{\frac{n_1!n_2!}{n'_1!n'_2!}} e^{-i\Phi_{m,s}(n'_1, n'_2)} e^{-it\hat{H}_{\text{eff}}}|n'_1, n'_2\rangle, \end{aligned} \quad (36)$$

where

$$\Phi_{m,s}(n'_1, n'_2) = s(\hat{H}_{\text{eff}}(n_1, n_2) - \hat{H}_{\text{eff}}(n'_1, n'_2)) \quad (37)$$

is a complex dynamical phase. The real part of $\Phi_{m,s}$ is the dynamical phase associated to the change in the atomic interaction energy because of the reduction of particles at time s . Since the Hamiltonian (3) is quadratic in the number operators \hat{n}_i , this real part is linear in n'_1 and n'_2 . Setting $N_1 = N_0 - r$ and $n'_2 = N_1 - n'_1$, one finds

$$\text{Re } \Phi_{m,s}(n'_1, n'_2) = \phi_m(s)n'_1 + c_m, \quad (38)$$

where $\phi_m(s)$ is given by Eq.(33) and c_m is an irrelevant n'_1 -independent phase. The imaginary part of $\Phi_{m,s}$ is associated to a change in the damping due to the reduction of particles at time s . It is quadratic in n'_i because of the presence of the cubic damping operator $\hat{D}_{3\text{-body}}$ (see Eq.(25)), but we will see that one can neglect the quadratic term under our assumption on the three-body loss rates. By neglecting all terms of order $sN_0\kappa_i$, $sN_0\kappa_{ij}$, $i, j = 1, 2$, $i \neq j$, and recalling that n'_1 and $n'_2 = N_1 - n'_1$ are at most of the order of N_0 , one gets

$$\begin{aligned} \text{Im } \Phi_{m,s}(n'_1, n'_2) &= -\frac{s}{2} \left[\sum_{i=1,2} \sum_{j \neq i} (3\kappa_i - 2\kappa_{ij} + \kappa_{ji})m_i \times \right. \\ &\quad \left. \left(n'_1 - \frac{N_1}{2} \right)^2 + (\delta_1 m_1 + \delta_2 m_2) \left(n'_1 - \frac{N_1}{2} \right) + G_m \right], \end{aligned} \quad (39)$$

where δ_i is given by Eq.(35) and

$$\begin{aligned} G_m &= \gamma_{12} \left(\frac{rN_1}{2} + m_1 m_2 \right) + \sum_{i=1,2} \left(\alpha_i + \gamma_i(N_1 - 1 + m_i) \right. \\ &\quad \left. + \sum_{j \neq i} (3\kappa_i + \kappa_{ji} + 2\kappa_{ij}) \frac{N_0^2}{4} \right) m_i. \end{aligned} \quad (40)$$

We now take as initial state the CS (1). The corresponding unnormalized wave function is obtained by using the Fock state expansion (2) and Eq.(36). This yields

$$\begin{aligned} |\tilde{\psi}_1(t)\rangle &= \frac{1}{2^{N_0/2}} \sqrt{\frac{N_0!}{N_1!}} \sum_{n'_1=0}^{N_1} \binom{N_1}{n'_1}^{1/2} e^{-it\hat{H}_{\text{eff}}} \\ &\quad e^{-i\Phi_{m,s}(n'_1, N_1 - n'_1)} |n'_1, N_1 - n'_1\rangle. \end{aligned} \quad (41)$$

Note that only the terms with $|n'_1 - N_1/2| \lesssim \sqrt{N_1}$ contribute significantly to the sum. Thus one can neglect the quadratic term in the right-hand side of Eq.(39) in the limit $N_0\kappa_i t, N_0\kappa_{ij} t \ll 1$. Plugging Eqs.(38) and (39)

into Eq.(41), one recognizes the Fock state expansion of a CS with N_1 atoms. We get

$$\begin{aligned} |\tilde{\psi}_1(t)\rangle &= 2^{-\frac{N_1}{2}} \sqrt{\frac{N_0!}{N_1!}} e^{-sG_m/2} \left[\cosh\left(\frac{s}{2} \sum_i \delta_i m_i\right) \right]^{\frac{N_1}{2}} \\ &\quad e^{-it\hat{H}_{\text{eff}}}|N_1; \theta_m(s), \phi_m(s)\rangle, \end{aligned} \quad (42)$$

in agreement with Eq.(32) above. Moreover, from Eqs.(22) and (42) we immediately obtain the probability $dp_m^{(t)}(s; 1)$ that a loss event of type m occurs in the time interval $[s, s + ds]$ and no other loss occur in $[0, t]$,

$$\begin{aligned} dp_m^{(t)}(s; 1) &= \tilde{p}_m^{(t)}(s; 1) \|e^{-it\hat{H}_{\text{eff}}}|N_1; \theta_m(s), \phi_m(s)\rangle\|^2 ds \\ \tilde{p}_m^{(t)}(s) &= \frac{\Gamma_m}{2^r} \frac{N_0!}{N_1!} e^{-sG_m} \cosh^{N_1} \left(\frac{s}{2} \sum_{i=1,2} \delta_i m_i \right). \end{aligned} \quad (43)$$

Let us assume that the BJJ is subject to r -body losses only, with $r = 1, 2$, or 3. According to Eq.(23), the density matrix in the subspace with $N_1 = N_0 - r$ atoms is

$$\begin{aligned} \hat{\rho}_{N_1}(t) &\propto \tilde{\rho}_{N_1}^{(1\text{-jump})}(t) = \sum_{m, |m|=r} \int_0^t ds \tilde{p}_m^{(t)}(s) \times \\ &\quad e^{-it\hat{H}_{\text{eff}}}|N_1; \theta_m(s), \phi_m(s)\rangle \langle N_1; \theta_m(s), \phi_m(s)| e^{it\hat{H}_{\text{eff}}}. \end{aligned} \quad (44)$$

The probability to measure N_1 atoms at time t reads $w_{N_1}(t) = \text{tr } \tilde{\rho}_{N_1}^{(1\text{-jump})}(t)$. Equation (44) means that by conditioning to a single loss event one obtains the same state as if there were no atom loss between times 0 and t , one had initially N_1 atoms, and the BJJ was subject to external θ - and ϕ -noises rotating the state around the Bloch sphere. More precisely, with the help of the commutation of \hat{H}_{eff} with the angular momentum operator $\hat{J}_z = (\hat{n}_1 - \hat{n}_2)/2$ and the identity $|N; \theta, \phi\rangle = (e^{i\phi} \cosh u)^{-N/2} e^{-i\phi + u} \hat{J}_z |N; \phi = 0\rangle$ with $u = \ln(\tan(\theta/2))$, one can rewrite this formula as

$$\begin{aligned} \tilde{\rho}_{N_1}^{(1\text{-jump})}(t) & \\ &\propto \sum_{m, |m|=r} \left\langle U_{\text{eff}}^{(m)}(s) |N_1; \phi = 0\rangle \langle N_1; \phi = 0| U_{\text{eff}}^{(m)}(t)^\dagger \right\rangle_s, \end{aligned} \quad (45)$$

where $U_{\text{eff}}^{(m)}(s) = e^{-i(\phi_m(s) + i \ln(\tan(\theta_m(s)/2)) \hat{J}_z} e^{-it\hat{H}_{\text{eff}}}$ is a non-unitary random evolution operator and the brackets denote the average with respect to the exponential distribution $f_m(s) \propto \Theta(t-s)e^{-sG_m}$ of the loss time s (here Θ denotes the Heaviside step function). Hence the effect of atom losses on the conditional state (44) with one loss event is equivalent to that of some θ - and ϕ -noises, in addition to the damping described in Sec. VI. These noises are characterized by the fluctuations

$$\begin{aligned} \delta\theta_m &\simeq \frac{1}{2} \delta s_m \left| \sum_{i=1,2} \delta_i m_i \right|, \quad \delta\phi_m = \delta s_m \left| \sum_{i=1,2} \chi_i m_i \right| \end{aligned} \quad (46)$$

(we assume here $\delta\theta_m \ll 1$), where δs_m is the fluctuation of the loss time with respect to the distribution

$\tilde{p}_m^{(t)}(s)\Theta(t-s)/\int_0^t ds \tilde{p}_m^{(t)}(s)$. This analogy between atom losses and ϕ -noise is already known in the literature in the weak loss regime [22]; in this regime the θ -noise is

negligible.

The density matrix (44) can be evaluated explicitly in the Fock basis. It reads

$$\langle n_1, n_2 | \tilde{\rho}_{N_1}^{(1\text{-jump})}(t) | n'_1, n'_2 \rangle \propto \sum_{m, |m|=r} \Gamma_m C_m(t; n_1, n'_1) \langle n_1, n_2 | \tilde{\rho}_{N_1}^{(\text{no loss})}(t) | n'_1, n'_2 \rangle \quad (47)$$

with

$$C_m(t; n, n') = \frac{1 - e^{-t[G_m + (\delta_1 m_1 + \delta_2 m_2)(n + n' - N_1)/2 + i(\chi_1 m_1 + \chi_2 m_2)(n - n')]} }{G_m + (\delta_1 m_1 + \delta_2 m_2)(n + n' - N_1)/2 + i(\chi_1 m_1 + \chi_2 m_2)(n - n')} . \quad (48)$$

In Eq.(47), $\tilde{\rho}_{N_1}^{(\text{no loss})}(t)$ denotes the unnormalized density matrix conditioned to no loss event between times 0 and t for an initial phase state with N_1 atoms,

$$\tilde{\rho}_{N_1}^{(\text{no loss})}(t) = e^{-it\hat{H}_{\text{eff}}} |N_1; \phi = 0\rangle \langle N_1; \phi = 0| e^{it\hat{H}_{\text{eff}}^\dagger}, \quad (49)$$

the matrix elements of which are given by Eq.(27) upon the replacement $N_0 \rightarrow N_1$. According to Eq.(47), the density matrix conditioned to a single loss event is the lossless density matrix $\hat{\rho}^{(0)}(t)$ for an initial phase state with $N_0 - r$ atoms, modulated by the envelope $\sum \Gamma_m C_m(t; n, n')$ and by the damping factor of Eq.(27).

Note that in the presence of both one-body and two-body losses, to get the state $\hat{\rho}_{N_0-2}(t)$ in the (N_0-2) -atom subspace one must add to $\hat{\rho}_{N_0-2}^{(1\text{-jump})}(t)$ the contribution of trajectories having two one-body loss events. In the next subsection we generalize the previous results to trajectories having more than one jump and determine the states $\hat{\rho}_N(t)$ for all N when the BJJ is subjected simultaneously to one-body, two-body, and three-body losses.

B. Contribution of trajectories with several loss events

The extension to $J > 1$ loss events of the calculation of the previous subsection does not present any difficulty. As before, we consider three-body loss rates satisfying $N_0 \kappa_i t, N_0 \kappa_{ij} t \ll 1$. Let us introduce the vector notation $\mathbf{s} = (s_1, \dots, s_J)$ for the sequence of loss times s_ν , with $0 \leq s_1 \leq \dots \leq s_J \leq t$, and $\mathbf{m} = (m_1, \dots, m_J)$ for the sequence of loss types $m_\nu = (m_{\nu,1}, m_{\nu,2})$, where $m_{\nu,i}$ is the number of atoms lost in the mode i during the ν th loss event. Finally, let $|\mathbf{m}| = \sum_{\nu=1}^J (m_{\nu,1} + m_{\nu,2})$ be the total number of atoms lost between times 0 and t . The wave function $|\psi_J(t)\rangle$ after J jumps of types \mathbf{m} occurring at times \mathbf{s} is still a time-evolved CS given by Eq.(32) upon replacing N_1 by $N_J = N_0 - |\mathbf{m}|$ and $\theta_m(s)$, $\phi_m(s)$ by the

random angles

$$\theta_{\mathbf{m}}(\mathbf{s}) = 2 \arctan \left(\exp \left\{ - \sum_{\nu=1}^J \frac{s_\nu}{2} (\delta_1 m_{\nu,1} + \delta_2 m_{\nu,2}) \right\} \right) \\ \phi_{\mathbf{m}}(\mathbf{s}) = \sum_{\nu=1}^J s_\nu (\chi_1 m_{\nu,1} + \chi_2 m_{\nu,2}), \quad (50)$$

where δ_i and χ_i are defined in Eqs.(34) and (35). As before, $\phi_{\mathbf{m}}(\mathbf{s})$ and $i \ln(\tan(\theta_{\mathbf{m}}(\mathbf{s})/2))$ are respectively the real and imaginary dynamical phases per atom in the first mode associated to the variations in the interaction energy and the damping following the particle losses.

We now assume that, in addition to the above condition on three-body losses, the two-body loss rates satisfy $t\gamma_i \ll 1$ and $t\gamma_{12} \ll 1$. It is shown in the Appendix D that the conditional states $\hat{\rho}_N(t)$ with $|N_0 - N| \ll N_0$ read in the Fock basis

$$\langle n_1, n_2 | \hat{\rho}_N(t) | n'_1, n'_2 \rangle \propto \mathcal{E}_N(t; n_1, n'_1) \langle n_1, n_2 | \tilde{\rho}_N^{(\text{no loss})}(t) | n'_1, n'_2 \rangle \quad (51)$$

with an envelop $\mathcal{E}_N(t; n, n')$ given in terms of the coefficients $C_m(t; n, n')$ of Eq.(48) by

$$\mathcal{E}_N(t; n, n') = \sum_{J_1, J_2, J_3 \geq 0, J_1 + 2J_2 + 3J_3 = N_0 - N} \frac{1}{J_1! J_2! J_3!} \\ \prod_{r=1}^3 \left[\sum_{|m|=r} \Gamma_m C_m(t; n, n') \right]^{J_r}. \quad (52)$$

Thus, $\mathcal{E}_N(t; n, n')$ is obtained by multiplying together the envelopes associated to single r -body loss events in Eq.(47) raised at the power J_r , and by summing over all the numbers J_r of r -body losses in the time interval $[0, t]$ such that $N = N_0 - J_1 - 2J_2 - 3J_3$.

Equations (32), (50), (51), and (52) are our main analytical results from the quantum trajectory approach. Let us recall that they are valid provided that $t\Gamma_m \ll N_0^{2-|m|}$ for all two-body ($|m| = 2$) and three-body ($|m| = 3$) loss rates Γ_m . This is not a strong restriction since the mean number $\langle \hat{N} \rangle_t$ of atoms in the BJJ at time t depends on the two-body and three-body loss rates like $N_0 \gamma_i t$ and

$N_0^2 \kappa_i t$ for large N_0 [43]. Hence the aforementioned condition is still fulfilled if a relatively large fraction (e.g. 50%) of the initial atoms are lost between time 0 and t by two-body and three-body processes.

In the next section, we use the above analytical results to explain the different decoherence scenarios discussed in Sec. V on the superpositions of phase states for symmetric and asymmetric loss rates and interaction energies.

VIII. CHANNEL EFFECTS AND PROTECTION OF QUANTUM CORRELATIONS AGAINST PHASE NOISE

We focus in this section on the conditional states with $N < N_0$ atoms at the time of formation $t = t_q$ of the macroscopic superpositions. To simplify the discussion, we assume in Subsections VIII A to VIII C that the BJJ is subject to r -body losses only (with $r = 1, 2$, or 3) and study the conditional density matrix $\hat{\rho}_{N_1}(t_q)$ with $N_1 = N_0 - r$ atoms, given by Eq.(44). The more general case of combined loss processes and more than one loss event is discussed in Subsection VIII D.

A. Results from the exact diagonalization method

Let us start by presenting the amount of QCs in the subspace with N_1 atoms calculated from the exact diagonalization method of appendix A. We restrict ourselves here to two-body losses, assuming no one-body, three-body, and inter-mode losses (i.e. $\alpha_i = \gamma_{12} = \kappa_i = \kappa_{ij} = 0$). The density matrix $\hat{\rho}_{N_1}(t_2)$ in the Fock basis is shown in Fig. 6. If the interaction energies in the two modes are equal, i.e. $U_1 = U_2$, we remark that $\hat{\rho}_{N_1}(t_2)$ is almost diagonal in the Fock basis for weak symmetric loss rates $\gamma_1 = \gamma_2 \lesssim \chi/N_0$ (upper left panel), while it has non vanishing off-diagonal elements at odd values of $n'_1 - n_1$ for completely asymmetric rates $\gamma_2 = 0$ (middle left panel). Moreover, if one takes a vanishing rate $\gamma_1 = 0$ in the first mode and tunes the energies such that $U_2 = U_{12}$, keeping $\chi = (U_1 + U_2 - 2U_{12})/2$ fixed, the density matrix has the same structure as that of a two-component superposition with $N_0 - 2$ atoms. This is confirmed by looking at the quantum Fisher information $F_{N_0-2}(t_2)$ in the subspace with $N_0 - 2$ atoms, which is displayed in Fig. 7. We stress that, unlike in Fig. 2, this Fisher information is not multiplied by the one-jump probability $w_{N_0-2}(t_q)$. If one of the modes does not lose atoms and $U_i = U_{12}$ in the other mode (Fig. 2b), $F_{N_0-2}(t_2)$ is approximately equal for $\gamma_1 \ll \chi/N_0$ to the Fisher information $(N_0 - 2)^2$ of a two-component superposition. At stronger loss rates $\gamma_1 \approx 1/T = \chi/(2\pi)$ it decreases to much lower values. In contrast, for symmetric losses and energies, $F_{N_0-2}(t_2)$ starts below the shot-noise limit at weak losses and increases with γ_1 to reach a maximum when $\gamma_1 \simeq 2/T$. As we will see below, these different behaviors of the Fisher information for symmetric and asymmetric loss rates and

energies occur in all subspaces with $N < N_0$ atoms and for all types of losses, thereby explaining the differences in the total Fisher information obtained in Sec. V. We show in the next subsection that this comes mainly from the combination of two effects: a channel effect and the reduction of phase noise in one loss channel by tuning the energies U_i .

B. Results from the quantum trajectory method for small loss rates

Let us concentrate on the small loss regime, i.e.

$$\Gamma_m \ll q\chi N_0^{1-r} \quad , \quad r = |m| = 1, 2, 3 . \quad (53)$$

In this case one can neglect the θ -noise since $\delta\theta_m$ is much smaller than the quantum fluctuations in the CSs forming the components of the superposition (6) (the latter are of the order of $1/\sqrt{N_0}$). In contrast, as follows from the large fluctuations $\delta s_m \approx t_q$ of the loss time s (which has an almost flat distribution between 0 and t_q ; see (43)), the ϕ -fluctuations are quite large. Actually, if $\chi_1 m_1 + \chi_2 m_2 \neq 0$ then $\delta\phi_m$ in Eq.(46) is of the order of the phase separation $\phi_{k+1,q} - \phi_{k,q} = 2\pi/q$ between the CSs.

The analytical results of Sec. VII take a simpler form in the limit (53). Due to Eq.(47), the conditional state $\hat{\rho}_{N_1}(t_q)$ in the Fock basis in the presence of r -body losses only is obtained by multiplying the matrix elements of the superposition of CSs by the damping factor

$$D(n_1, n'_1) = e^{-\frac{\pi}{\chi q}(d_{N_1}(n_1) + d_{N_1}(n'_1))} \quad (54)$$

and by the envelope

$$\mathcal{E}_{q,r}(n_1, n'_1) = \frac{q\chi}{\pi} \sum_{|m|=r} \Gamma_m C_m(t_q; n_1, n'_1) . \quad (55)$$

For symmetric energies $U_1 = U_2$, i.e. $\chi_1 = -\chi_2 = \chi$, the coefficient $C_m(t_q; n, n')$ in Eq.(48) can be approximated by

$$C_m(t_q; n, n') \simeq \frac{1 - \exp\left\{-i\frac{\pi}{q}(m_1 - m_2)(n - n')\right\}}{i\chi(m_1 - m_2)(n - n')} . \quad (56)$$

The factor in front of the sum in (55) is put for convenience (then $\mathcal{E}_{q,r}(n_1, n_1) = \sum_{|m|=r} \Gamma_m$) and disappears in the state normalization. We discuss below three important effects of atom losses on the atomic state, by analyzing the form of the envelope (55) for various loss rates and energies.

1. Complete phase relaxation for $U_1 = U_2$

Let us first study the impact of the phase noise on $\hat{\rho}_{N_1}(t_q)$ for *symmetric interaction energies* $U_1 = U_2$. Then $\delta\phi_m \approx |m_1 - m_2|\pi/q$, implying that phase noise due to losses with unequal numbers of atoms m_i in each

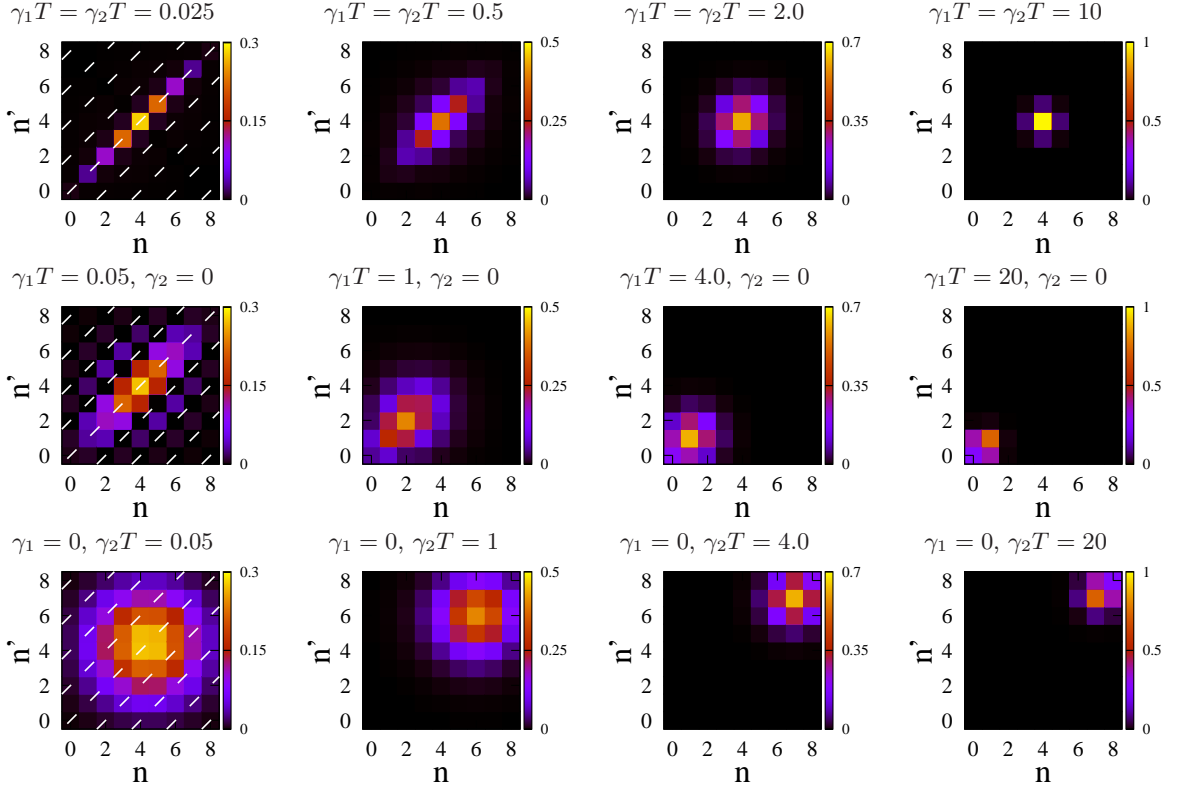


FIG. 6. (Color online) Moduli $|\langle n, N_0 - 2 - n | \hat{\rho}_{N_0-2}(t_2) | n', N_0 - 2 - n' \rangle|$ of the density matrix in the Fock basis at time $t_2 = T/4$ in the subspace with $(N_0 - 2)$ atoms for increasing two-body losses rates (from left to right), from the exact diagonalization method. The upper panels correspond to symmetric losses and interaction energies ($\gamma_1 = \gamma_2$ and $U_1 = U_2$), the middle panels to asymmetric losses and symmetric energies ($\gamma_2 = 0$ and $U_1 = U_2$), and the bottom panels to asymmetric losses and energies ($\gamma_1 = 0$ and $U_2 = U_{12}$). The revival time T is the same in all cases. White dashed lines are marking the values of (n, n') for which the matrix elements of the diagonal part $[\hat{\rho}^{(0)}(t_2)]_d$ of the two-component superposition do not vanish. Other parameters: $N_0 = 10$, $\alpha_i = \gamma_{12} = \kappa_i = \kappa_{ij} = 0$.

mode i blurs out the phases of the CSs, whereas a loss of one atom in each mode does not modify the state.

Before showing this explicitly, let us mention some results established in [18, 20] concerning the effect of phase noise on superpositions of CSs in BJJs. Recall that one can decompose the density matrix as a sum of its diagonal and off-diagonal parts defined in Eq.(9). This can also be done in the presence of noise. Phase noise flattens the Husimi distribution of the superposition in the ϕ direction (phase relaxation), which manifests itself by the convergence for strong noise of the diagonal part of the density matrix to a statistical mixture of Fock states with completely undefined phases. A second effect of phase noise is the loss of the coherences between the CSs of the superposition, leading to a convergence of the off-diagonal part to zero at strong noises. This off-diagonal part, albeit it does not influence the Husimi distribution, contains the QCs useful for interferometry. It was pointed out in [18, 20] that for intermediate phase noise one may have almost complete phase relaxation while some QCs remain (weak decoherence).

In our case, the action of phase noise on the diagonal and off-diagonal parts of $\hat{\rho}_{N_1}(t_q)$ can be evaluated

exactly. By Eqs.(10) and (47), the matrix elements of $[\hat{\rho}_{N_1}(t_q)]_d$ vanish for $n'_1 \neq n_1$ modulo q . We may thus restrict our attention to $n'_1 = n_1 + pq$ for integer p 's. Due to Eqs.(55) and (56), if $p \neq 0$ then

$$\mathcal{E}_{q,r}(n_1, n_1 + pq) \simeq \begin{cases} -i\Delta\alpha \frac{1-(-1)^p}{\pi p} & \text{for } r = 1 \\ \gamma_{12} & \text{for } r = 2 \\ -i(\Delta\kappa + 3\Delta\kappa_{12}) \frac{1-(-1)^p}{3\pi p} & \text{for } r = 3 \end{cases} \quad (57)$$

with $\Delta\alpha = \alpha_2 - \alpha_1$, $\Delta\kappa = \kappa_2 - \kappa_1$, and $\Delta\kappa_{12} = \kappa_{21} - \kappa_{12}$. Therefore, for two-body losses and in the absence of inter-mode losses $\gamma_{12} = 0$, the diagonal part is equal to a statistical mixture of Fock states in the limit (53),

$$\langle n_1, N_1 - n_1 | [\hat{\rho}_{N_1}(t_q)]_d | n'_1, N_1 - n'_1 \rangle \propto \delta_{n_1, n'_1} \binom{N_1}{n_1} e^{-\frac{\pi}{\chi q} d_{N_1}(n_1)}. \quad (58)$$

This is confirmed in the upper and middle left panels in Fig. 6, where one observes vanishing matrix elements on the dashed lines $n'_1 = n_1 \pm 2$, $n'_1 = n_1 \pm 4, \dots$. We thus find that the loss of two atoms in the same mode leads to complete phase relaxation. This explains

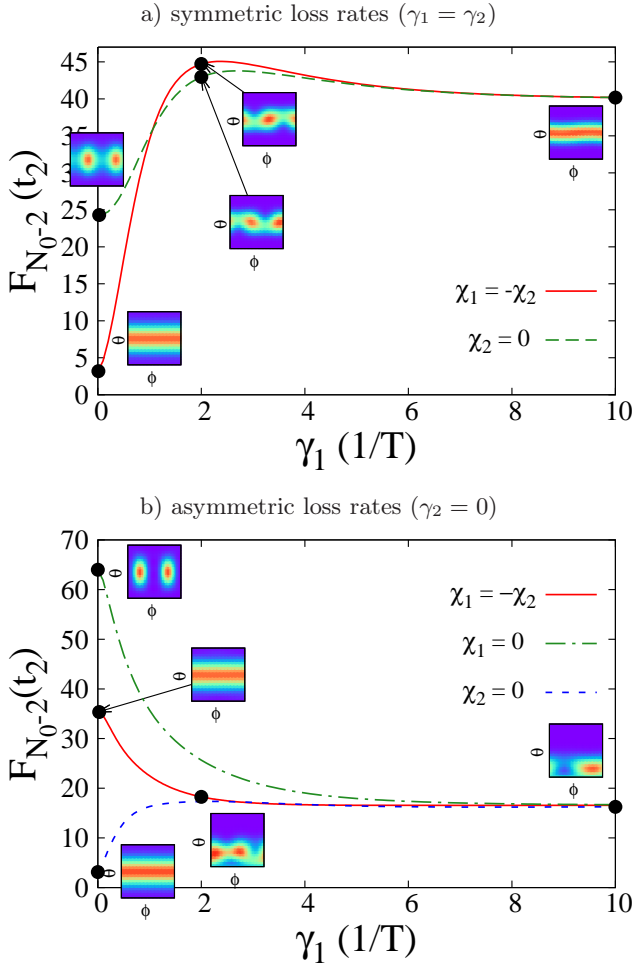


FIG. 7. (Color online) Quantum Fisher information optimized in the subspace with $(N_0 - 2)$ atoms at time t_2 as a function of the two-body loss rate (in unit of T^{-1}), from exact diagonalization, for (a) symmetric losses $\gamma_1 = \gamma_2$ with $U_1 = U_2$ (red solid line) and $U_2 = U_{12}$ (green dashed line); (b) completely asymmetric losses with $\gamma_2 = 0$ and $U_1 = U_2$ (red solid line), $U_1 = U_{12}$ (green dot dashed line), and $U_2 = U_{12}$ (blue dashed line). The U_i are chosen in such a way that the revival time T does not change. Insets: plots of the Husimi functions for some specific choices of loss rates (indicated by circles and arrows in the figures). Other parameters as in Fig. 6.

the ϕ -independent profile of the Husimi distributions in the insets in Fig. 7 corresponding to $\chi_1 = -\chi_2$ and $\gamma_1 \ll 1/(TN_0)$. In contrast, no phase relaxation occurs in the inter-mode channel $m = (1, 1)$. For one- and three-body losses, complete phase relaxation occurs for symmetric losses ($\alpha_1 = \alpha_2$, $\kappa_1 = \kappa_2$, and $\kappa_{12} = \kappa_{21}$) only. This can be understood intuitively as follows. For weak rates the random phase $\phi_{1,0} = s\chi$ ($\phi_{0,1} = -s\chi$) produced by the loss of one atom in the mode $i = 1$ ($i = 2$) is uniformly distributed in $[0, \pi/q]$ ($[-\pi/q, 0]$). Since the components of the superposition have a phase separation of $2\pi/q$, it is clear that one needs equal loss probabilities in the two modes to wash out its phase content com-

pletely. Note that here complete phase relaxation comes from an exact cancellation when adding the contributions of the two loss channels $m = (1, 0)$ and $m = (0, 1)$, which separately lead to non-diagonal matrices $[\hat{\rho}_{N_1}(t_q)]_d$. A similar argument applies to three-body losses.

2. Loss of quantum correlations when $U_1 = U_2$: channels effects

As discussed above, the phenomenon of phase relaxation does not tell us anything about the QCs useful for interferometry, which can still be present in the atomic state even if one has complete phase relaxation. Let us now study these QCs, contained in the off-diagonal part $[\hat{\rho}_{N_1}(t_q)]_{od}$ of the conditional state. We still assume symmetric energies $U_1 = U_2$. This off-diagonal part corresponds to the matrix elements of $\hat{\rho}_{N_1}(t_q)$ in the Fock basis such that $n'_1 \neq n_1$ modulo q (see Eq.(10)). For weak losses satisfying (53) the main effect of phase noise is, in view of Eq.(56), to multiply the matrix elements in the absence of noise by a factor $(n_1 - n'_1)^{-1}$. This factor decays to zero as one moves away from the diagonal but does not modify substantially the elements close to the diagonal. This explains the presence of off-diagonal matrix elements for $n'_1 = n_1 \pm 1$ and $n'_1 = n_1 \pm 3$ for two-body loss rates $\gamma_1 \ll \chi/N_0$ and $\gamma_2 = 0$ and equal energies in Fig. 6 (left middle panel), as well as the relatively high value of the Fisher information $F_{N_0-2}(t_2)$ in Fig. 7(b). For such loss rates and energies we are in the noise regime of the aforementioned weak decoherence, i.e. phase noise is more efficient in washing out the phase content of each component of the superposition than in destroying the coherences.

However, we see in Figs. 6 and 7 that the situation is quite different for symmetric two-body losses in the two modes, $\gamma_1 = \gamma_2$ and $\gamma_{12} = 0$: then the off-diagonal part of $\hat{\rho}_{N_1}(t_2)$ vanishes completely and the Fisher information at small losses is smaller than N_0 . This comes from a cancellation when adding the contributions of the $m = (2, 0)$ and $m = (0, 2)$ loss channels, which occurs only at time t_2 and in the absence of inter-mode losses. A similar cancellation occurs at time t_3 when the two modes are subject to three-body losses with symmetric rates $\kappa_1 = \kappa_2$ and $\kappa_{12} = \kappa_{21} = 0$. In fact, for such loss rates Eqs.(55) and (56) yield $\mathcal{E}_{r,r}(n, n') \simeq 2\Gamma_{r,0}\delta_{n,n'}$ for $r = 2, 3$. Therefore, $[\hat{\rho}_{N_0-2}(t_2)]_{od} = 0$, so that not only the diagonal part but the whole density matrix $\hat{\rho}_{N_0-2}(t_2)$ is diagonal in the Fock basis and given by Eq.(58) (upper left panel in Fig. 6). As a consequence of this channel effect, the two-component (three-component) superposition suffers when $\gamma_{12} = 0$ ($\kappa_{12} = \kappa_{21} = 0$) from a *complete decoherence* in the N_1 -atom subspace for any small symmetric two-body (three-body) loss rates. Such a channel effect does of course not occur for completely asymmetric losses involving only one channel. It is illustrated in Fig. 8, which displays the Fisher information $F_{N_0-2}(t)$ as a function of time. For asymmetric two-body losses,

$F_{N_0-2}(t)$ is maximum at the two-component superposition time t_2 as in the lossless case. For symmetric two-body losses, instead, $F_{N_0-2}(t)$ is minimum at t_2 due to the channel effect.

Note that symmetric one-body losses $\alpha_1 = \alpha_2$ or inter-mode three-body losses $\kappa_{12} = \kappa_{21}$ do not produce any channel effect. This means that these loss processes are less detrimental to macroscopic superpositions than symmetric two-body losses. For instance, one has $\mathcal{E}_{q,1}(n, n') = 2\alpha_1 \text{sinc}[\pi(n-n')/q]$ for $\alpha_1 = \alpha_2$ (we remind that we are treating for the moment the case of symmetric interactions $U_1 = U_2$). A striking consequence of this observation will be discussed in Sec. VIII D 1.

3. Protecting macroscopic superpositions by tuning the interaction energies U_i

Let us now turn to the case of *asymmetric interaction energies* $U_1 \neq U_2$. We will see that tuning these energies makes possible a further reduction of decoherence for all kinds of loss processes. In order to keep the formation time $t_q = \pi/(\chi q)$ of the superposition constant, we vary U_1 and U_2 while fixing $2\chi = \chi_1 - \chi_2$. We still consider weak losses satisfying (53). Then phase relaxation described above is incomplete, as well as decoherence at times t_2 or t_3 for symmetric losses. An interesting situation is $U_2 = U_{12} < U_1$, i.e. $\chi_2 = 0$ and $\chi_1 = 2\chi$. Then $\phi_{0,r}(s) = 0$ by Eq.(33), thus the second mode is protected against phase noise, whereas the first mode is subject to a strong noise with fluctuations $\delta\phi_{r,0} \approx 2\pi r/q$. Taking for instance vanishing inter-mode rates, one gets from Eqs.(55) and (48)

$$\mathcal{E}_{q,r}(n, n') = \Gamma_{0,r} + q\Gamma_{r,0} \frac{1 - \exp\{-i\frac{2\pi r}{q}(n - n')\}}{2i\pi r(n - n')}. \quad (59)$$

For symmetric rates $\Gamma_{0,r} = \Gamma_{r,0}$, the off-diagonal matrix elements of $\hat{\rho}_{N_1}(t_2)$ in the Fock basis coincide with those of a two-component superposition up to a factor $\approx 1/2$. Loosely speaking, $\hat{\rho}_{N_1}(t_2)$ is a ‘‘half macroscopic superposition’’. Such a state has a large Fisher information, as shown in Fig. 7(a). An even larger Fisher information is obtained for completely asymmetric losses such that atoms are lost only in the protected mode $i = 2$, i.e. $\Gamma_{r,0} = 0$. Then $\mathcal{E}_{q,r}(n, n') = \Gamma_{0,r}$ and $\hat{\rho}_{N_1}(t_q) \propto \hat{\rho}_{N_1}^{(\text{no loss})}(t_q)$, that is, the conditional state $\hat{\rho}_{N_1}(t_q)$ coincides with a macroscopic superposition of q CSs with $N_1 = N_0 - r$ atoms, slightly modified by the damping factor (54). This is in agreement with the convergence at weak losses and asymmetric energies of the Fisher information $F_{N_0-2}(t_2)$ in Fig 7(b) to the highest possible value $(N_0 - 2)^2$, and to the presence of two well-pronounced peaks at $\phi = \pm\pi/2$ in the corresponding Husimi distributions.

In conclusion, by tuning the interaction energies U_i such that $\chi_1 = 0$ or $\chi_2 = 0$ one can protect one mode against phase noise, to the expense of enlarging noise

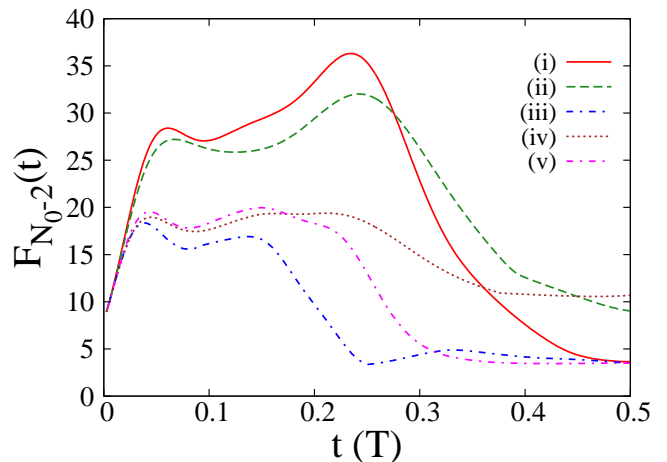


FIG. 8. (Color online) Quantum Fisher information optimized in the subspace with $N_0 - 2$ atoms versus time for symmetric energies $U_1 = U_2$, from exact diagonalization. The red solid and green dashed lines (upper curves) correspond to asymmetric two-body losses with (i) $\gamma_1 T = 0.05$, $\gamma_2 = 0$ and (ii) $\gamma_1 T = 1.0$, $\gamma_2 = 0$. The blue dot-dashed, brown dotted and magenta dot-dashed lines (lower curves) correspond to symmetric two- and one-body losses with (iii) $\gamma_1 = \gamma_2 = 0.025/T$, $\alpha_i = 0$, (iv) $\gamma_1 = \gamma_2 = 0.5/T$, $\alpha_i = 0$, and (v) $\gamma_1 = \gamma_2 = 0.025/T$, $\alpha_1 = \alpha_2 = 0.5/T$. Other parameters: $N_0 = 10$ and $\gamma_{12} = \kappa_i = \kappa_{ij} = 0$.

in the other mode, thereby limiting decoherence effects on the conditional state with N_1 atoms. This way of ‘‘switching-off’’ phase noise in one mode has been pointed out in [21] for two-body losses. We find here that it applies to one- and three-body losses as well.

C. Intermediate and strong loss rates

To complete the description of Fig. 7 we now discuss three effects of atom losses occurring at larger rates Γ_m violating (53). Let us warn the reader, however, that these effects on the conditional state with N_1 atoms do not affect the total density matrix, because of the small probability to have a single loss event between $t = 0$ and $t = t_q$ at strong losses.

1. Increasing the loss rates reduces phase noise

Let us first study the regime of intermediate loss rates. Surprisingly, the ϕ -noise *decreases* if one increases Γ_m . This results from the decrease of the loss time fluctuations δs_m at increasing Γ_m , leading to a decrease of the phase fluctuations $\delta\phi_m$ in Eq.(33). In fact, while for small rates the loss time is uniformly distributed on the interval $[0, t_q]$ and thus $\delta s_m \approx t_q$, for larger rates the loss has more chance to occur at small times and δs_m gets smaller. For instance, it is easy to see on the unnormalized distribution (43) that $\delta s_m \simeq G_m^{-1}$ when $G_m \gtrsim \chi q$

and $N_0 \gg 1$, where G_m is a non-decreasing function of Γ_m , see Eq.(40). This decreasing of phase noise sets in for $G_m \approx \chi q$, that is, $\Gamma_m \approx \chi q N_0^{1-|m|}$. Note that the approximations leading to Eqs.(51) and (52) are still justified at such loss rates. Therefore, by increasing the loss rates one protects the conditional state with N_1 atoms against phase noise and thus against decoherence. As seen in Fig. 2, this counter-intuitive effect does not manifest itself in the total Fisher information $F_{\text{tot}}(t)$. Indeed, when increasing γ_1 the subspaces contributing to the total Fisher information (16) involve less atoms and hence have less QCs, and the increase of $F_{N_0-2}(t)$ is counter-balanced by the decrease of the probability $w_{N_0-2}(t)$. As a consequence, $F_{\text{tot}}(t)$ is getting smaller.

2. Effect of the θ -noise

The fact that the peaks of the Husimi distributions in Fig. 7(b) at intermediate losses are centered at values of θ smaller than $\pi/2$ is due to the θ -noise. In fact, in this figure $\delta_1 = 2\gamma_1 > 0$ and $\delta_2 = 0$, so that $\theta_{2,0}(s) < \pi/2$ and $\theta_{0,2}(s) = \pi/2$. For larger initial atom numbers N_0 the θ -noise is always small, its fluctuations being of the order of $1/N_0$ when $N_0 \gg 1$. Actually, when $G_m \gtrsim \chi q$ one finds $\delta\theta_m \approx 1/N_0$ by replacing δs_m by G_m^{-1} in Eq.(46), whereas for $G_m < \chi q$ one has $\delta\theta_m < t_q r \max\{|\delta_1|, |\delta_2|\}/2$.

3. Damping effects

Increasing further the rates Γ_m , the damping due to the effective Hamiltonian in Eq.(44) begins to play the major role. The combination of this damping with the reduced phase noise effect described above leads again to different behaviors of $F_{N_1}(t_q)$ as a function of the loss rates for symmetric and asymmetric losses. Let us recall from Sect.VI that the onset of damping is at $\Gamma_m \approx \chi q N_0^{1-|m|}$ in the symmetric case and $\Gamma_m \approx \chi q N_0^{-|m|}$ in the completely asymmetric case. On the other hand, we have seen above that phase noise reduction begins when $\Gamma_m \approx \chi q N_0^{1-|m|}$. For symmetric losses, there thus exists a small range of loss rates Γ_m on which phase noise is reduced by increasing Γ_m while the damping is still relatively small. This explains the increase of $F_{N_1}(t_2)$ with γ_1 seen in Fig. 7(a). At the point where $F_{N_1}(t_2)$ reaches a maximum, two peaks are clearly visible in the Husimi distribution, as opposed to the flat distribution observed at weak losses. This nicely illustrates phase-noise reduction. In contrast, in the asymmetric case damping effects counter-balance phase-noise reduction when increasing γ_1 and the Fisher information decreases (even though some peaks show up in the Husimi plots). For $\gamma_1 = \gamma_2 \gg \chi$ and even N_0 , $\hat{\rho}_{N_1}(t_q)$ converges to a Fock state with $(N_0 - 2)/2$ atoms in each mode, which has a high Fisher information $(N_0 - 2)N_0/2$ (see Appendix C). For strong asymmetric losses, instead, $\hat{\rho}_{N_1}(t_q)$ converges

to a superposition of Fock states with $n_1 = 0$ or 1 atom in the first mode, and $F_{N_1}(t_2) \approx N_0$, as seen in Fig. 7(b). Similarly, the comparison of the two first rows in Fig. 6 shows that an increase of $\gamma_1 = \gamma_2$ makes non-vanishing off-diagonal matrix elements to appear, as a consequence of phase-noise reduction, while for $\gamma_2 = 0$ the same operation moves the peak in the density matrix towards $n_1 = n'_1 = 0$ as a consequence of damping.

We remind once more that these effects at strong losses concern the conditional state with N_1 atoms, characterized by a small probability $w_{N_1}(t_q)$. Note also that the approximations made in Sec. VII break down for such losses, namely, Eq.(51) is still valid but the envelope $\mathcal{E}(t; n_1, n'_1)$ has a more complex expression than that given in Eq.(52) (see Appendix D). Since for $\Gamma_m \gg \chi N_0^{1-|m|}$ the most important effect is damping, the precise form of $\mathcal{E}(t, n_1, n'_1)$ does, however, not matter.

D. Conditional states for several loss events

We finally extend the previous results to the case of several loss events. In view of Eq.(52) most of the physical effects discussed above are present in all subspaces with N atoms, $0 < N_0 - N \ll N_0$.

1. Reduction of channel effect due to one-body losses

The channel effect leading to complete decoherence at times t_2 or t_3 for weak symmetric losses (see Sec. VIII B 2) is suppressed if, in addition to two- or three-body losses, also one-body losses are present. The argument goes as follows. The density matrix in the subspace with $N_1 = N_0 - r$ atoms, $r = 2$ or 3, is given by Eq.(51) with an envelope $\mathcal{E}_{N_1}(t_r; n, n') \propto \mathcal{E}_{r,r}(n, n') + [\mathcal{E}_{r,1}(n, n')]^r/r!$, see Eq.(52). As pointed out in above, $\mathcal{E}_r(n, n')$ vanishes for $n \neq n'$ (channel effect), but this is not the case for the envelope $\mathcal{E}_{r,1}(n, n')$ coming from one-body losses. We therefore find that by adding one-body losses one can reduce decoherence on the two-component or three-component superposition. We have checked that off-diagonal elements indeed appear in the density matrix $\hat{\rho}_{N_0-2}(t_2)$ in the Fock basis shown in the upper left panel in Fig.6 when one adds one-body losses. A surprising consequence of these off-diagonal elements is shown in Fig.8: if one-body losses are added, we observe an increase of the Fisher information $F_{N_0-2}(t_2)$ with respect to the case with two-body losses only.

2. Tuning interaction energies

For strongly asymmetric loss rates, it is possible to protect the QCs in the atomic state after many loss events by tuning the interaction energies while keeping fixed the energy χ governing the lossless dynamics, as in the case of a single loss event (see Sec.VIII B 3). However, if the

loss rates are symmetric, decoherence is strong for any choice of the energies. The argument goes as follows. If the one-, two-, and three-body losses occur mostly in the same mode i , one can switch phase noise off in that mode i by tuning the atomic energies using Feshbach resonances in such a way that $\chi_i = 0$, as explained in Sec. VIII B 3. Then each conditional state $\hat{\rho}_N(t_q)$ is close to a q -component superposition of CSs with N atoms apart from small damping effects (this is due to the form (52) of the envelope $\mathcal{E}(t; n, n')$ in Eq.(51) for $N_0 - N \ll N_0$ and to the fact that $\mathcal{E}_{q,r}(n, n')$ is almost constant for weak loss rates $\Gamma_m \ll q\chi N_0^{1-|m|}$). The same result holds if losses occur mainly via inter-mode two-body processes (i.e. $\gamma_{12} \gg \gamma_i, \alpha_i/N_0, \kappa_i N_0, \kappa_{ij} N_0$); then one must tune the energies such that $U_1 = U_2$. For symmetric losses the situation is different. As soon as the number $N_0 - N$ of lost atoms becomes large the tuning of the energies U_i is inefficient to keep the coherences of the superposition. This is due to the fact that the probability that all losses occur in the same mode decreases exponentially with the number of loss events, and we have seen that only one mode can be protected against phase noise if χ is kept constant. Therefore, when a large number of atoms leave the system, the loss rates must be strongly asymmetric in order to be able to protect efficiently QCs from decoherence by tuning the U_i . These results provide a good explanation the effects described in Figs. 2 and 3 (Sec. V).

In order to fully explain the high values of the total Fisher information at time t_q for strongly asymmetric losses, we must show that the interferometer direction \vec{n} optimizing the Fisher information $F(\hat{\rho}_N(t_q), \hat{J}_{\vec{n}})$ in the N -atom subspace is almost the same for all subspaces (otherwise one could not take advantage of the QCs to improve the phase precision in interferometry, except when the number of atoms at time t_q is known exactly). To see that this is indeed the case, let us note that these directions roughly coincide with one of the phases $\phi_{k,q}$ of the superposition of CSs with N atoms, which are given by (we assume here $E_1 = E_2$)

$$\phi_{k,q} = [2k + \delta_q - N + \chi^{-1}(N-1)(U_2 - U_1)/2] \frac{\pi}{q} \quad (60)$$

with $\delta_q = 0$ if q is even and 1 otherwise. When $U_2 = U_{12}$ (or $U_1 = U_{12}$), we obtain $\phi_{k,q} = [2k + \delta_q - 2N + 1]\pi/q$ (or $\phi_{k,q} = [2k + \delta_q - 1]\pi/q$). Thus the components of the superposition are transformed one into another by changing N . One deduces from this argument that the total Fisher information $F_{\text{tot}}(t_q)$ in Eq.(16) is close to the Fisher information of a q -component superposition with $\langle \hat{N} \rangle_{t_q}$ atoms, and thus scale like $\langle N \rangle_{t_q}^2$, where $\langle \hat{N} \rangle_{t_q}$ is the average number of atoms at time t_q .

IX. SUMMARY AND CONCLUDING REMARKS

We have studied in detail the decoherence induced by one-, two- and three-body atom losses on the macroscopic superpositions of CSs dynamically generated in BJJs. For all loss types and at weak losses, two effects degrade the superposition state at most. These effects are a strong effective phase noise and a channel effect. The latter effect gives rise to enhanced decoherence on the two-component (three-component) superposition after summing over all the loss channels when the two-body (three-body) loss rates and interaction energies are the same in the two modes of the junction and the inter-mode loss rates vanish. Conversely, if all losses occur mainly in one mode we have shown that, by exploiting the experimental tunability of the interaction energies, it is possible to partially prevent this degradation by adjusting the interaction energy U_i of each mode, keeping their sum fixed. More precisely, the effective phase noise can be suppressed in the mode losing more atoms by choosing an interaction energy in this mode equal to the inter-mode interaction U_{12} . For instance, in internal BJJs and for the Rubidium atoms used in Ref. [13], this could be done by taking a non-zero value of the inter-mode scattering length a_{12} and by reducing the scattering length a_1 in the mode $i = 1$ losing less atoms. Then, because a_2 and a_{12} are almost equal, one has $U_2 \simeq U_{12}$, whereas $U_1 - U_{12}$ can be large. For experimentally relevant loss rates and initial atom numbers, we have found that the amount of coherence left at the time of formation of the two-component superposition can be made in this way substantially higher, provided that the system has strongly asymmetric losses (see Fig. 3). In the experiment of Ref. [13], this condition is met for two-body losses but not for one-body losses, which are symmetric in the two modes. As a consequence, in the range of parameters mimicking the experimental situation [13] that we have studied, we predict that one-body loss processes lead to much stronger decoherence effects on the macroscopic superpositions than the asymmetric two- or three-body processes.

ACKNOWLEDGMENTS

We are grateful to K. Rzażewski, F.W.J. Hekking, P. Treutlein, and M.K. Oberthaler for helpful discussions. K.P. acknowledges support by the Polish Government Funds N N202 174239 for the years 2010-2012 and financial support of the project ‘‘Decoherence in long range interacting quantum systems and devices’’ sponsored by the Baden-Württemberg Stiftung. D.S acknowledges support from the French ANR project no. ANR-09-BLAN-0098-01 and A.M. from the ERC ‘‘Handy-Q’’ grant N. 258608.

Appendix A: Solution of the master equation by the exact diagonalization method

We present in this appendix the exact solution of the master equation (11) with Lindblad generators (12) in the absence of inter-mode losses. In the notation of Sec. II this means $\kappa_{21} = \kappa_{12} = \gamma_{12} = 0$. The loss rates in the first and second modes are denoted as in Sec. IV by $\Gamma_{r,0}$ and $\Gamma_{0,r}$, respectively, with $r = 1, 2$, and 3 for one-, two-, and three-body losses.

Let us first note that the inter-mode interaction energy $U_{12}\hat{n}_1\hat{n}_2$ in the Bose-Hubbard Hamiltonian (3) can be absorbed in the intra-mode interactions up to a term depending on the total number operator \hat{N} only, yielding

$$\begin{aligned}\hat{H}_0 &= \hat{H}^{(1)} + \hat{H}^{(2)} + \frac{U_{12}}{2}\hat{N}(\hat{N} - 1) \\ \hat{H}^{(i)} &= E_i\hat{n}_i + \frac{U_i - U_{12}}{2}\hat{n}_i(\hat{n}_i - 1), \quad i = 1, 2.\end{aligned}\quad (\text{A1})$$

As neither the initial density operator nor the dynamics couple subspaces with distinct total atom numbers, one can ignore the term depending on \hat{N} . Then \hat{H}_0 reduces to a sum of two single-mode Hamiltonians $\hat{H}^{(1)}$ and $\hat{H}^{(2)}$. Since we assumed no inter-mode losses, the Lindblad generators can also be expressed as sums of generators acting on single modes. Thus the two modes are not coupled in the master equation (11) and the dynamics of the two-mode BEC can be deduced from that of two independent single-mode BEC, which are only coupled in the initial state $\hat{\rho}(0) = |\psi(0)\rangle\langle\psi(0)|$ given by Eq. (1).

Let us first focus on the single-mode master equation:

$$\frac{d\hat{\rho}}{dt} = -i[\hat{H}, \hat{\rho}(t)] + \sum_{r=1}^3 \mathcal{L}_{r\text{-body}}(\hat{\rho}(t)) \quad (\text{A2})$$

with $\hat{H} = \frac{U}{2}(\hat{a}^\dagger)^2\hat{a}^2$ and

$$\mathcal{L}_{r\text{-body}}(\hat{\rho}) = \Gamma_r \hat{a}^r \hat{\rho} (\hat{a}^\dagger)^r - \frac{\Gamma_r}{2} \{ (\hat{a}^\dagger)^r \hat{a}^r, \hat{\rho} \}, \quad (\text{A3})$$

where we denote the energies $U_1 - U_{12}$ or $U_2 - U_{12}$ collectively by U and the loss rates $\Gamma_{r,0}$ and $\Gamma_{0,r}$ collectively by Γ_r . Hereafter we use the notation

$$\rho_{k,l+j}^{k+j,l} = \langle k, l+j | \hat{\rho} | k+j, l \rangle \quad (\text{A4})$$

for the matrix elements of the two-mode density matrix in the Fock basis, and similarly

$$\rho_k^{k+j} = \langle k | \hat{\rho} | k+j \rangle \quad (\text{A5})$$

in the single-mode case. This unusual indexing will turn out to be convenient later. The master equation (A2) takes the following form in the Fock basis:

$$\frac{d}{dt}\rho_k^{k+j} = \lambda_{j,k} \rho_k^{k+j}(t) + \sum_{r=1}^3 u_{j,k+r}^{(r)} \rho_{k+r}^{k+r+j}(t), \quad (\text{A6})$$

where we have set $\rho_l^{l+j}(t) = 0$ for $l > N_0$ or $l+j > N_0$,

$$\begin{aligned}\lambda_{j,k} &= -\frac{iU}{2} \left(k(k-1) - (k+j)(k+j-1) \right) \\ &\quad - \sum_{r=1}^3 \frac{\Gamma_r}{2} \left(\prod_{w=0}^{r-1} (k-w) + \prod_{w=0}^{r-1} (k+j-w) \right),\end{aligned}\quad (\text{A7})$$

and

$$u_{j,k}^{(r)} = \Gamma_r \prod_{w=0}^{r-1} \sqrt{(k-w)(k+j-w)}. \quad (\text{A8})$$

From (A6) we conclude that (A2) couples only the matrix elements which are in the same distance j from the diagonal. Therefore, the set of differential equations (A6) for all j and k can be grouped into families of equations with a fixed j , which can be solved independently from each other.

For a given j and $N = j, \dots, N_0$, we solve Eq.(A6) with the initial condition

$$\rho_k^{k+j}(0) = \delta_{k, N-j}, \quad k = 0, \dots, N-j. \quad (\text{A9})$$

Then $\rho_k^{k+j}(t) = 0$ at all times t when $k > N-j$. It is convenient to group the matrix elements together into a vector with k th component given by $\rho_k^{k+j}(t)$,

$$\mathbf{v}_{N,j}(t) = \left(\rho_0^j(t), \rho_1^{1+j}(t), \dots, \rho_{N-j}^N(t) \right). \quad (\text{A10})$$

Then the equations (A6) for different k but fixed j can be combined into a single equation for the vector $\mathbf{v}_{N,j}$:

$$\frac{d\mathbf{v}_{N,j}}{dt} = A_{N,j} \mathbf{v}_{N,j}(t), \quad (\text{A11})$$

where $A_{N,j}$ is a time-independent $(N-j+1) \times (N-j+1)$ triangular superior matrix with coefficients determined by (A6). The solution of Eq.(A11) has the form

$$\mathbf{v}_{N,j}(t) = \exp(A_{N,j}t) \mathbf{v}_{N,j}(0). \quad (\text{A12})$$

To determine the exponential in the right-hand side one has to diagonalize $A_{N,j}$.

As this matrix is triangular, its eigenvalues are given by its diagonal elements $\lambda_{j,n}$ defined in Eq.(A7). Let $\mathbf{l}_{j,n}$ and $\mathbf{p}_{j,n}$ be left and right eigenvectors of the non-Hermitian matrix $A_{N,j}$ with the eigenvalue $\lambda_{j,n}$. In the general case we were not able to find explicit formulas for these eigenvectors. However, thanks to Eq.(A6) their components $p_{j,n}^k$ and $l_{j,n}^k$, $k = 0, 1, \dots, N-j$, can be obtained recursively thanks to the formulas

$$p_{j,n}^k = \begin{cases} 0 & \text{if } k > n \\ 1 & \text{if } k = n \\ \frac{u_{j,k+1}^{(1)} p_{j,n}^{k+1} + u_{j,k+2}^{(2)} p_{j,n}^{k+2} + u_{j,k+3}^{(3)} p_{j,n}^{k+3}}{\lambda_{j,n} - \lambda_{j,k}} & \text{if } k < n \end{cases} \quad (\text{A13})$$

and

$$l_{j,n}^k = \begin{cases} \frac{u_{j,k}^{(1)} l_{j,n}^{k-1} + u_{j,k}^{(2)} l_{j,n}^{k-2} + u_{j,k}^{(3)} l_{j,n}^{k-3}}{\lambda_{j,n} - \lambda_{j,k}} & \text{if } k > n \\ 1 & \text{if } k = n \\ 0 & \text{if } k < n \end{cases}. \quad (\text{A14})$$

Using these eigenvectors and eigenvalues, the solution (A12) with initial condition (A9) takes the form

$$\mathbf{v}_{N,j}(t) = \sum_{n=0}^{N-j} l_{j,n}^{N-j} \mathbf{p}_{j,n} e^{\lambda_{j,n} t}. \quad (\text{A15})$$

Having the solution in a single mode, we can find the solution of the two-mode master equation (11),

$$\begin{aligned} \rho_{k,l+j}^{k+j,l}(t) &= \sum_{N=k+j}^{N_0-l} \rho_{N-j,N_0-N+j}^{N,N_0-N} (0) \\ &\times [\mathbf{v}_{N,j}^{(1)}(t)]_k [\mathbf{v}_{N_0-N+j,j}^{(2)}(t)]_l^*, \end{aligned} \quad (\text{A16})$$

where we added superscripts to the vectors $\mathbf{v}_{N,j}(t)$ to refer to the two modes 1 and 2, in order to stress that the loss rates and interaction energies differ between modes.

The solutions (A15) and (A16) can be substantially simplified if only one-body losses are present. For instance Eq.(A15) takes the form

$$\begin{aligned} [\mathbf{v}_{N,j}(t)]_k &= \quad (\text{A17}) \\ &= e^{z_j t} e^{k x_j t} \binom{N-j}{k}^{\frac{1}{2}} \binom{N}{k+j}^{\frac{1}{2}} \left(\frac{e^{x_j t} - 1}{x_j / \Gamma_1} \right)^{N-k-j} \end{aligned}$$

with $z_j = iU(j^2 - j)/2 - \Gamma_1 j/2$ and $x_j = iUj - \Gamma_1$.

Although the formula for any density matrix element (A16) is a bit cumbersome, one can use it to derive simple expressions for the correlation functions characterizing the state. To give an example, the first-order correlation function ($j = 1$) reads (for simplicity we take symmetric loss rates $\Gamma_{1,0} = \Gamma_{0,1} = \alpha$ and energies $U_1 = U_2 = U_{12} + \chi$):

$$\begin{aligned} G^1(t) &= \text{Re} \left\{ \langle \hat{a}_2^\dagger \hat{a}_1 \rangle_t \right\} \\ &= \text{Re} \left\{ \sum_{k,l} \rho_{k,l+1}^{k+1,l}(t) \sqrt{k+1} \sqrt{l+1} \right\} = \frac{N_0 e^{-\alpha t}}{2} \times \\ &\quad \left(\frac{\alpha^2 + \chi^2 e^{-\alpha t} \cos(\chi t) + \alpha \chi e^{-\alpha t} \sin(\chi t)}{\chi^2 + \alpha^2} \right)^{N_0-1}. \end{aligned}$$

The latter formula agrees with the results obtained with the help of the quantum trajectory method in [16] and the generating functions in [17].

In the case of two- and three-body losses, the eigenvectors $\mathbf{p}_{j,n}$ and $l_{j,n}$ are evaluated numerically using the recurrences formulas (A13) and (A14).

Appendix B: Extraction of experimentally relevant parameters

We choose a symmetric trap with frequency $\omega = 2\pi \times 500\text{Hz}$ and initial number of atoms $N_0 = 100$ as in [14]. We compute the condensate wave function $\psi(\mathbf{r})$ with the help of the Gross-Pitaevskii equation, assuming no inter-species interaction, i.e. $a_{12} = 0$, and neglecting the interactions in one of the two modes, namely $a_2 = 0$, where a_{12} and a_2 are the corresponding scattering lengths. Then $U_2 = U_{12} = 0$. We estimate the interaction energy in the second mode with the formula $U_1 = \frac{4\pi a_1}{M} \int |\psi|^4(\mathbf{r}) d^3r$, M being the atomic mass. To compute the loss rates we use the constants for the atomic species used in [12, 16]. For such parameters the probability of three-body collisions is relatively small compared with the probability of two-body processes, the latter being highly asymmetric. Conversely, in the experiment one-body losses appear to act symmetrically in the two modes. For the results shown in Fig. 3 we additionally neglect inter-mode losses (i.e. $\gamma_{12} = 0$).

Appendix C: Conditional state with N_0 atoms in the strong loss regime

In the strong loss regime $\Gamma_m t \gg 1$, the probability $w_{N_0}(t)$ that the BJJ does not lose any atom in the time interval $[0, t]$ is very small (see Eq.(28)). As a consequence, the contribution to the total density matrix $\hat{\rho}(t)$ of the conditional state $\hat{\rho}_{N_0}(t)$ with N_0 atoms is negligible. However, one can gain some insight on QCs at intermediate loss rates by studying this strong loss regime. This study is performed in this appendix. We also discuss the form of the damping factor in Eq.(27) for asymmetric three-body loss rates.

Let us first consider *symmetric three-body losses* $\kappa_1 = \kappa_2$ and $\kappa_{12} = \kappa_{21}$ and assume that Eq.(29) defines an effective loss rate $a > 0$. The strong loss regime then corresponds to $at \gg 1$. The damping factor in Eq.(27) is Gaussian and given by Eq.(30). After renormalization by $w_{N_0}(t)$, this damping factor send all the matrix elements $\langle n_1, N_0 - n_1 | \hat{\rho}_{N_0}(t) | n'_1, N_0 - n'_1 \rangle$ of $\hat{\rho}_{N_0}(t)$ to zero except those for which n_1 and n'_1 are the closest integer(s) to \bar{n}_1 . If \bar{n}_1 is a half integer, the four matrix elements with $n_1, n'_1 = \bar{n}_1 \pm 1/2$ are damped by exactly the same factor. Therefore, $\hat{\rho}_{N_0}(t)$ converges to a pure state,

$$\hat{\rho}_{N_0}(t) \rightarrow |\psi_0^{(\infty)}(t)\rangle \langle \psi_0^{(\infty)}(t)|, \quad (\text{C1})$$

which is either a Fock state $|\psi_0^{(\infty)}\rangle = |E(\bar{n}_1), N_0 - E(\bar{n}_1)\rangle$ if \bar{n}_1 is not half integer (here $E(\bar{n}_1)$ denotes the closest integer to \bar{n}_1) or, if \bar{n}_1 is half integer, a superposition of two Fock states

$$\begin{aligned} |\psi_0^{(\infty)}(t)\rangle &\propto \sum_{\pm} \binom{N_0}{\bar{n}_1 \pm \frac{1}{2}}^{1/2} e^{it\varphi_{\pm}} \\ &|\bar{n}_1 \pm \frac{1}{2}, N_0 - \bar{n}_1 \mp \frac{1}{2}\rangle \end{aligned} \quad (\text{C2})$$

with $\varphi_+ = E_2 + (N_0 - \bar{n}_1 - \frac{1}{2})U_2 + (2\bar{n}_1 - N_0)U_{12}$ and $\varphi_- = E_1 + (\bar{n}_1 - \frac{1}{2})U_1$. In particular, if $\gamma_1 = \gamma_2$ and $\alpha_1 = \alpha_2$ (case (i) in Sec. VI), $\hat{\rho}_{N_0}(t)$ converges to the Fock state $|\psi_0^{(\infty)}\rangle = |\frac{N_0}{2}, \frac{N_0}{2}\rangle$ if N_0 is even and to a superposition of the Fock states $|\frac{N_0 \pm 1}{2}, \frac{N_0 \mp 1}{2}\rangle$ if N_0 is odd (since $\bar{n}_1 = N_0/2$). Similarly, if $\gamma_2 = \gamma_{12} = \kappa = 0$ (case (ii) in Sec. VI), $\hat{\rho}_{N_0}(t)$ converges to the Fock state $|0, N_0\rangle$ if $\alpha_2 < \alpha_1$ (since then $\bar{n}_1 < 1/2$, see Eq.(31)) and to a superposition of Fock states with $n_1 = 0$ or 1 atoms in the first mode if $\alpha_1 = \alpha_2$ (since then $\bar{n}_1 = 1/2$). Ignoring one-body losses, this can be explained as follows. If one detects the same number of atoms initially and at time $t \gg 1/\gamma_1$, the atomic state must have zero or one atom in the first mode suffering from two-body losses (otherwise one would expect the BJJ to have lost some atoms at time t).

Let us turn to the case $a < 0$, i.e. $\gamma_{12} > \gamma_1 + \gamma_2 + 2(N_0 - 2)\kappa$ (case (iii) in Sec. VI). We still assume symmetric three-body losses. It is easy to show from Eq.(31) that $\bar{n}_1 > N_0/2$ if and only if $\Delta\gamma < -\Delta\alpha/(N_0 - 1)$. Therefore, $\hat{\rho}_{N_0}(t)$ converges in the strong loss limit $|a|t \gg 1$ to the Fock state with $n_1 = 0$ (respectively $n_1 = N_0$) atoms in the first mode if $\Delta\gamma < -\Delta\alpha/(N_0 - 1)$ (respectively $\Delta\gamma > -\Delta\alpha/(N_0 - 1)$), whereas it converges to the so-called NOON state

$$|\psi_0^{(\infty)}(t)\rangle = \frac{1}{\sqrt{2}} \left(e^{-itN_0[E_1 + U_1(N_0 - 1)/2]} |N_0, 0\rangle + e^{-itN_0[E_2 + U_2(N_0 - 1)/2]} |0, N_0\rangle \right) \quad (C3)$$

if $\Delta\gamma = -\Delta\alpha/(N_0 - 1)$. The latter state arises because from the knowledge that the BJJ has not lost any atom at time $t \gg |a|^{-1}$ one can be confident to have either $n_1 = 0$ or $n_1 = N_0$ atom in the first mode, in such a way that no inter-mode two-body collision is possible. Since one cannot decide among the two possibilities, the state of the BJJ is the superposition (C3).

If $a = 0$, i.e. $\gamma_{12} = \gamma_1 + \gamma_2 + 2(N_0 - 2)\kappa$, then

$$d_{N_0}(n_1) - d_{N_0}(0) = bn_1 \quad (C4)$$

varies linearly with n_1 , with $b = -(\Delta\alpha + (N_0 - 1)\Delta\gamma)/2$ (we use here the same notation as in Sec. VI). One easily finds that in the strong loss limit $|b|t \gg 1$, $\hat{\rho}_{N_0}(t)$ converges to the same states as in the previous case $a < 0$.

Note that for $\Delta\gamma = -\Delta\alpha/(N_0 - 1)$ one has no damping, i.e. $\hat{\rho}_{N_0}(t)$ coincides with the lossless density matrix.

Let us now investigate the *asymmetric three-body loss case* $K = 3(\kappa_1 - \kappa_2 + \kappa_{21} - \kappa_{12})/2 \neq 0$ for arbitrary loss rates. Without loss of generality we may assume $K > 0$ (otherwise one can permute the two modes). The damping factor in Eq.(27) is cubic in n_1 ,

$$d_{N_0}(n_1) = \frac{1}{3}Kn_1^3 + an_1^2 + bn_1 + c, \quad (C5)$$

where c an irrelevant n_1 -independent constant and

$$a = \frac{1}{2} [\gamma_1 + \gamma_2 - \gamma_{12} - 3\kappa_1 + 3(N_0 - 1)\kappa_2 + (N_0 + 1)\kappa_{12} - (2N_0 - 1)\kappa_{21}] \quad (C6)$$

$$b = \frac{1}{2} [-\Delta\alpha + \Delta\gamma - N_0(2\gamma_2 - \gamma_{12}) - 2\Delta\kappa + N_0(-3(N_0 - 2)\kappa_2 - \kappa_{12} + (N_0 - 1)\kappa_{21})] \quad (C7)$$

In the last expression we have set $\Delta\kappa = \kappa_2 - \kappa_1$. The minimum of $d_{N_0}(n_1)$ over all integers n_1 between 0 and N_0 is reached either for $n_1 = 0$ or for $n_1 = \bar{n}_1 = (\sqrt{a^2 - bK} - a)/K$. The effect of damping at time t_q on the lossless density matrix sets when $|K|N_0^3$, $|a|N_0^2$ or $|b|N_0$ are of the order of χq or larger, i.e. for loss rates $\kappa \gtrsim \chi q/N_0^3$, $\gamma \gtrsim \chi q/N_0^2$, or $\alpha \gtrsim \chi q/N_0$. For completely asymmetric losses of all kinds (i.e. all rates vanish save for α_1 , γ_1 , and κ_1) one finds $\bar{n}_1 = 1 + 1/\sqrt{3}$ when only κ_1 is nonzero and $\bar{n}_1 \simeq (-\gamma_1 + \sqrt{\gamma_1^2 - 3\kappa_1\alpha_1})/(3\kappa_1) < 0$ when $N_0 \gg 1$ and α_1 , $N_0\gamma_1$, and $N_0^2\kappa_1$ have the same order of magnitude. In both cases, $\hat{\rho}_{N_0}(t)$ converges at strong losses to the Fock state $|0, N_0\rangle$, in analogy with what happens for two-body losses.

Appendix D: Generalization of the calculation of Sec. VII for the conditional state $\hat{\rho}_N(t)$

We derive in this appendix the formulas (51) and (52) for the density matrix $\hat{\rho}_N(t)$ in the subspace with N atoms, with $0 < N_0 - N \ll N_0$.

Let us first determine the unnormalized wave function $|\tilde{\psi}_J(t)\rangle$ after J jumps of types m_1, \dots, m_J occurring at times $0 \leq s_1 \leq \dots \leq s_J \leq t$. We assume $t\kappa_i N_0 \ll 1$, $t\kappa_{ij} N_0 \ll 1$, and $J \ll N_0$. Using the vector notation of Sec. VII B, an easy (but somehow tedious) generalization of the calculation leading to Eq.(42) yields

$$|\tilde{\psi}_J(t)\rangle = 2^{-\frac{|m|}{2}} \sqrt{\frac{N_0!}{N_J!}} \exp\left\{-\frac{1}{2} \sum_{\nu=1}^J s_\nu G_{m,\nu}\right\} \left[\cosh\left(\sum_{\nu=1}^J \frac{s_\nu}{2} \sum_{i=1,2} \delta_i m_{\nu,i}\right) \right]^{\frac{N_J}{2}} e^{-it\hat{H}_{\text{eff}}} |N_J; \theta_{\mathbf{m}}(\mathbf{s}), \phi_{\mathbf{m}}(\mathbf{s})\rangle, \quad (D1)$$

where $N_J = N_0 - |\mathbf{m}|$ is the number of atoms left in the BJJ after the J loss events (i.e. $|\mathbf{m}| = \sum_\nu |m_\nu|$ with

$|m_\nu| = \sum_i m_{\nu,i}$ the number of atoms lost in the ν th event), the angles $\theta_{\mathbf{m}}(\mathbf{s})$ and $\phi_{\mathbf{m}}(\mathbf{s})$ are given by Eq.(50), and

$$G_{\mathbf{m},\nu} = \sum_{i=1,2} \left[\alpha_i + \gamma_i(N_J - 1 + \mu_{\nu,i} + \mu_{\nu+1,i}) + \sum_{j \neq i} (3\kappa_i + \kappa_{ji} + 2\kappa_{ij}) \frac{N_0^2}{4} \right] m_{\nu,i} + \gamma_{12} \left(\frac{|m_\nu| N_J}{2} + \mu_{\nu,1} \mu_{\nu,2} - \mu_{\nu+1,1} \mu_{\nu+1,2} \right) \quad (\text{D2})$$

with $\mu_{\nu,i} = \sum_{\nu'=1}^J m_{\nu',i}$ for $\nu = 1, \dots, J$ and $i = 1, 2$.

We now determine the unnormalized density matrix $\tilde{\rho}_N(t)$ in the subspace with N atoms. Due to Eqs.(23) and (D1), its matrix elements in the Fock basis are

$$\langle n_1, n_2 | \tilde{\rho}_N(t) | n'_1, n'_2 \rangle = \sum_{J=1}^{N_0} \sum_{\mathbf{m}, N_0 - |\mathbf{m}| = N} \Gamma_{m_1} \dots \Gamma_{m_J} \int_{0 \leq s_1 \leq \dots \leq s_J \leq t} ds_1 \dots ds_J \langle n_1, n_2 | \tilde{\psi}_J(t) \rangle \langle \tilde{\psi}_J(t) | n'_1, n'_2 \rangle \propto \mathcal{E}_N(t; n_1, n'_1) \langle n_1, n_2 | \tilde{\rho}_N^{(\text{no loss})}(t) | n'_1, n'_2 \rangle, \quad (\text{D3})$$

where $\tilde{\rho}_N^{(\text{no loss})}(t)$ is the conditional state with N atoms for an initial state $|\psi(0)\rangle = |N; \phi = 0\rangle$, see (49), and

$$\mathcal{E}_N(t; n, n') = \sum_{J=1}^{N_0} \int_{0 \leq s_1 \leq \dots \leq s_J \leq t} ds_1 \dots ds_J \sum_{\mathbf{m}, N_0 - |\mathbf{m}| = N} \Gamma_{m_1} \dots \Gamma_{m_J} \exp \left\{ -i(n - n') \sum_{\nu=1}^J s_\nu \sum_i \chi_i m_{\nu,i} \right\} \times \exp \left\{ - \sum_{\nu=1}^J s_\nu G_{\mathbf{m},\nu} - (n + n' - N_J) \sum_{\nu=1}^J \frac{s_\nu}{2} \sum_i \delta_i m_{\nu,i} \right\}. \quad (\text{D4})$$

We now show that in the limit $t\gamma_i, t\gamma_{12} \ll 1$ and for $1 \leq J \ll N_0$, the envelope $\mathcal{E}_N(t; n, n')$ takes the particularly simple form given by Eq.(52). Actually, in this limit the expression (D2) of $G_{\mathbf{m},\nu}$ reduces to the corresponding

expression (40) for a single loss event of type $m = m_\nu$,

$$G_{\mathbf{m},\nu} \simeq G_{m_\nu} \simeq \gamma_{12} \frac{|m| N_0}{2} + \sum_{i=1,2} \left(\alpha_i + \gamma_i N_0 + \sum_{j \neq i} (3\kappa_i + \kappa_{ji} + 2\kappa_{ij}) \frac{N_0^2}{4} \right) m_{\nu,i}. \quad (\text{D5})$$

The integrand in Eq.(D4) is then symmetric under the exchange of the s_ν 's, allowing us to replace the integration range by $[0, t]^J$ upon division by $J!$. With the help of a simple counting argument, one obtains Eq.(52).

-
- [1] U. Fano, Phys. Rev. **124**, 1866 (1961).
[2] H. Feshbach, Annals of Physics **5**, 357 (1958).
[3] I. Bloch, Nature Physics **1**, 23 (2005).
[4] I. Bloch, Nature **453**, 1016 (2008).
[5] C. Weitenberg, M. Endres, J. F. Sherson, M. Cheneau, P. Schauss, T. Fukuhara, I. Bloch, and S. Kuhr, Nature **471**, 319 (2011).
[6] M. Kitagawa and M. Ueda, Phys. Rev. A **47**, 5138 (1993).
[7] A. S. Sørensen and K. Mølmer, Phys. Rev. Lett. **86**, 4431 (2001).
[8] A. Sørensen, L. M. Duan, J. I. Cirac, and P. Zoller, Nature **409**, 63 (2001).
[9] B. Yurke and D. Stoler, Phys. Rev. Lett. **57**, 13 (1986).
[10] D. Stoler, Phys. Rev. D **4**, 2309 (1971).
[11] J. Esteve, C. Gross, A. Weller, S. Giovanazzi, and M. K. Oberthaler, Nature **455**, 1216 (2008).
[12] F. Riedel, P. Böhi, Y. Li, T. W. Hänsch, A. Sinatra, and P. Treutlein, Nature **464**, 1170 (2010).
[13] C. Gross, T. Zibold, E. Nicklas, J. Estève, and M. K. Oberthaler, Nature **464**, 1165 (2010).
[14] A. Sinatra and Y. Castin, Eur. Phys. J. D **4**, 247 (1998).
[15] Y. Li, Y. Castin, and A. Sinatra, Phys. Rev. Lett. **100**, 210401 (2008).
[16] L. Yun, P. Treutlein, J. Reichel, and A. Sinatra, Eur. Phys. J. B **68**, 365 (2009).
[17] K. Pawłowski and K. Rzażewski, Phys. Rev. A **81**, 013620 (2010).
[18] G. Ferrini, D. Spehner, A. Minguzzi, and F. W. J. Hekking, Phys. Rev. A **84**, 043628 (2011).
[19] Y. P. Huang and M. G. Moore, Phys. Rev. A **73**, 023606 (2006).
[20] G. Ferrini, D. Spehner, A. Minguzzi, and F. W. J. Hekking, Phys. Rev. A **82**, 033621 (2010).

- [21] K. Pawłowski, D. Spehner, A. Minguzzi, and G. Ferrini, Phys. Rev. A **88**, 013606 (2013).
- [22] A. Sinatra, J.-C. Dornstetter, and Y. Castin, Front. Phys **7**, 86 (2012).
- [23] S. L. Braunstein and C. M. Caves, Phys. Rev. Lett. **72**, 3439 (1994).
- [24] W. M. Zhang, D. H. Feng, and R. Gilmore, Rev. Mod. Phys. **62**, 867 (1990).
- [25] G. Milburn, J. Corney, E. Wright, and D. Walls, Phys. Rev. A **55**, 4318 (1997).
- [26] J. Anglin, Phys. Rev. Lett. **79**, 6 (1997).
- [27] M. W. Jack, Phys. Rev. Lett. **89**, 140402 (2002).
- [28] M. W. Jack, Phys. Rev. A **67**, 043612 (2003).
- [29] A. Itah, H. Veksler, O. Lahav, A. Blumkin, C. Moreno, C. Gordon, and J. Steinhauer, Phys. Rev. Lett. **104**, 113001 (2010).
- [30] C. Gross, J. Estève, M. K. Oberthaler, A. D. Martin, and J. Ruostekoski, Phys. Rev. A **84**, 011609 (2011).
- [31] D. B. Hume, I. Stroescu, M. Joos, W. Muessel, H. Strobel, and M. K. Oberthaler, Phys. Rev. Lett. **111**, 253001 (2013).
- [32] B. Yurke, S. L. McCall, and J. R. Klauder, Phys. Rev. A **33**, 4033 (1986).
- [33] L. Pezze and A. Smerzi, Phys. Rev. Lett. **102**, 100401 (2009).
- [34] P. Hyllus, L. Pezzé, and A. Smerzi, Phys. Rev. Lett. **105**, 120501 (2010).
- [35] P. Hyllus, O. Gühne, and A. Smerzi, Phys. Rev. A **82**, 012337 (2010).
- [36] H. Carmichael, *An Open System Approach to Quantum Optics* (Springer-Verlag, New York, 1991).
- [37] K. Mølmer, Y. Castin, and J. Dalibard, J. Opt. Soc. Am. B **10**, 524 (1993).
- [38] V. P. Belavkin, Journal of Mathematical Physics **31**, 2930 (1990).
- [39] A. Barchielli and V. P. Belavkin, Journal of Physics A: Mathematical and General **24**, 1495 (1991).
- [40] M. Plenio and P. Knight, Rev. Mod. Phys. **70**, 101 (1998).
- [41] S. Haroche and J.-M. Raimond, *Exploring the Quantum: Atoms, Cavities, and Photons* (Oxford University Press, Oxford, 2006).
- [42] C. Gross, J. Phys. B **45**, 103001 (2012).
- [43] If BJJ is subject to symmetric two-body (respectively three-body) losses only, the phenomenological rate equations give $\langle \hat{N} \rangle_t \simeq N_0(\gamma_1 N_0 t + 1)^{-1}$ (respectively $\langle \hat{N} \rangle_t \simeq N_0(2\kappa_1 N_0^2 t + 1)^{-1/2}$) for $N_0 \gg 1$.